

## **General Disclaimer**

### **One or more of the Following Statements may affect this Document**

- This document has been reproduced from the best copy furnished by the organizational source. It is being released in the interest of making available as much information as possible.
- This document may contain data, which exceeds the sheet parameters. It was furnished in this condition by the organizational source and is the best copy available.
- This document may contain tone-on-tone or color graphs, charts and/or pictures, which have been reproduced in black and white.
- This document is paginated as submitted by the original source.
- Portions of this document are not fully legible due to the historical nature of some of the material. However, it is the best reproduction available from the original submission.

**NASA TECHNICAL  
MEMORANDUM**

**NASA TM X- 73,190**

**NASA TM X-73,190**

**SYMPOSIUM ON RECENT RESULTS IN INFRARED ASTROPHYSICS**

**Ames Research Center  
Moffett Field, California 94035**

**(NASA-TM-X-73190) SYMPOSIUM ON RECENT  
RESULTS IN INFRARED ASTROPHYSICS (NASA)  
84 p HC A05/MF A01**

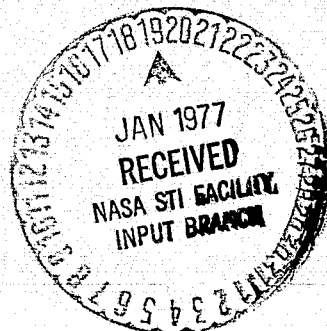
**CSCL 03B**

**N77-15955**

**Unclas**

**G3/90 59633**

**January 1977**



1. Report No. NASA TM X-73,190	2. Government Accession No.	3. Recipient's Catalog No.	
4. Title and Subtitle SYMPOSIUM ON RECENT RESULTS IN INFRARED ASTROPHYSICS*		5. Report Date	
		6. Performing Organization Code	
7. Author(s) Edited by Palmer Dyal		8. Performing Organization Report No. A-6856	
		10. Work Unit No. 188-41-55-01	
9. Performing Organization Name and Address Ames Research Center Moffett Field, Calif. 94035		11. Contract or Grant No.	
		13. Type of Report and Period Covered Technical Memorandum	
12. Sponsoring Agency Name and Address National Aeronautics and Space Administration Washington, D.C. 20546		14. Sponsoring Agency Code	
		15. Supplementary Notes *Sponsored by Ames Research Center, NASA, and American Astronomical Society.	
16. Abstract  <p>This publication contains the abstracts of papers presented at a symposium titled "Recent Results in Infrared Astrophysics" held at Ames Research Center in January 1977.</p> <p>The abstracts emphasize photometric, spectroscopic, polarization, and theoretical results on a broad range of current topics in infrared astrophysics.</p>			
17. Key Words (Suggested by Author(s)) Infrared      Airborne      Stars Astrophysics      Balloon      Planets Telescope      Cryogenics      Galaxy Detector      Nebulae		18. Distribution Statement  Unlimited  STAR Category - 90	
19. Security Classif. (of this report) Unclassified	20. Security Classif. (of this page) Unclassified	21. No. of Pages 84	22. Price* \$4.75

SYMPOSIUM ON  
RECENT RESULTS IN INFRARED ASTROPHYSICS  
JANUARY 1977  
AMES RESEARCH CENTER

TABLE OF CONTENTS

	<u>Page</u>
I. SOLAR SYSTEM OBJECTS	1
1. Inference of the Atmospheric Structure of Jupiter and Saturn from Their Far Infrared Spectra by T. Encrenaz and M. Combes.	2
2. Far Infrared Spectrophotometry of the Giant Planets by E.F. Erickson, D. Goorvitch, J.P. Simpson, and D.W. Strecker.	6
3. Fundamentals of PH <sub>3</sub> and NH <sub>3</sub> in the Infrared: Current Pursuits in Laboratory Spectroscopy by K. N. Rao.	9
4. Preliminary Measurements of the Emission Spectrum of the Zodiacal Cloud by D.A. Briotta and J.R. Houck.	12
II. STELLAR SOURCES	13
1. The Effects of Winds and Coronas of Hot Stars on the Infrared and Radio Continua by J.P. Cassinelli and L. Hartmann.	14
2. Spectrophotometry of Early-Type Stars from 1.2 to 4.2 Microns by J.D. Scargle, F.C. Witteborn, D.W. Strecker, and E.F. Erickson.	15
3. 0.85 to 2.5 Micron Spectrum of $\gamma$ Cassiopeia by M.F. Campbell and R.I. Thompson.	16
4. Aircraft and Ground Based Infrared Spectroscopy of MWC 349, MWC 297 and Lk H $\alpha$ 101 by R.I. Thompson, E.F. Erickson, D.W. Strecker, and F.C. Witteborn.	17
5. Spectral Observations of Eta Carina at 4-Microns by D.K. Aitken, B. Jones, J.D. Bregman, D.F. Lester, and D.M. Rank.	19
6. Airborne Photometric Observations between 1.25 and 3.25 $\mu$ of Late-Type Stars by G.C. Augason, H.L. Nordh, and S.G. Olofsson.	20
7. Infrared Narrow Band Spectrophotometry of Molecular Bands in Late Type Stars by C.P. Rinsland, R.F. Wing, and R.R. Joyce.	23
8. Observations of First-Overtone Silicon Monoxide Bands in Cool Stars by R.F. Wing, C.P. Rinsland, and R.R. Joyce.	26

	<u>Page</u>
9. Airborne Infrared Spectra (2900-5600 $\text{cm}^{-1}$ of Stars and Planets by L.L. Smith and T. Hilgeman.	29
10. Spectrophotometry of OH 26.5 + 0.6 by W.J. Forrest, F.C. Gillett, J.R. Houck, J. McCarthy, K.M. Merrill, J.L. Pipher, R.C. Puetter, R.W. Russell, B.T. Soifer, and S.P. Willner.	32
11. The Spectrum of IRC 10216 from 2.0 to 8.5 Microns by F.C. Witteborn, D.W. Strecker, E.F. Erickson, S.M. Smith, and J.H. Goebel.	35
III. NEBULAE	37
1. Hydrodynamic Calculation of Collapsing Interstellar Clouds by H. Gerola, and A.E. Glassgold.	38
2. The Calculated Infrared Appearance of Collapsing Protostellar Clouds by H.W. Yorke.	40
3. Density and Temperature Gradients in SGR B2, by L.J. Caroff.	43
4. An Interpretation of the Becklin-Neugebauer Object and Related Infrared Point Sources by P.J. Bedijn, H.J. Habing, and T. de Jong.	44
5. The Energetics of Molecular Clouds by N.J. Evans II, G.N. Blair, and S. Beckwith.	47
6. Strong Far Infrared Emission from a Compact Source in S140 by P.M. Harvey, M.F. Campbell, and W.F. Hoffmann.	48
7. Far Infrared Observations of Molecular Cloud S140 and the Galactic Plane by D. Rouan, P. Lena, J.L. Puget, K. De Boer, and J. Wijnbergen.	49
8. Discovery of a Far Infrared Source in W45 with a New Balloon-Borne Helium-Cooled 0.4-meter Telescope by M.F. Campbell, P.M. Harvey, W.F. Hoffmann, M.R. Jacobson, D.B. Ward, M.O. Harwit, and P.A. Aannestad.	52
9. Fabry-Perot Observations of the SIII, $^1D_2 - ^3P_1$ Transition, at 9069 Å in the Orion Nebula by H. Olthof and C.B. Cosmovici.	53
10. High Resolution Mapping of the Orion Nebula Region at 30, 50, and 100 Microns by M.W. Werner, E.E. Becklin, I. Gatley, and G. Neugebauer.	55
11. Far Infrared Lamellar Grating Observations of Jupiter and HII Regions by J.L. Pipher, J.G. Duthie, and M.P. Savedoff.	56

	<u>Page</u>
12. Medium Resolution Spectroscopy of NGC 7027 From 16 to 38 Microns by J. McCarthy, W. Forrest, and J.R. Houck.	57
13. 4-8 $\mu$ Spectrophotometric Observations of NGC 7027 and M82 by R.W. Russell, B.T. Soifer, and S.P. Willner.	58
14. Origin of 40-350 Micron Flux in Sources Associated with HII Regions by J.P. Emerson.	61
15. Infrared Emission and Properties of Dust of Gaseous Nebula by V. Petrosian, R.A. Dana, and L.J. Caroff.	62
16. On the Energy Balance of the Infrared Radiation in Planetary Nebulae, Galactic and Extragalactic HII Regions by K.V.K. Iyengar and K.S. Krishna Swamy.	64
IV. GALAXIES	69
1. Airborne Far Infrared Observations of the Galactic Center Region by I. Gatley, E.E. Becklin, M.W. Werner, and C.G. Wynn-Williams.	70
2. Preliminary Results of a Balloon-Borne Observation of the Far Infrared Galactic Diffuse Emission Between $l=38^{\circ}$ and $l=55^{\circ}$ by G. Serra, J.L. Puget, and C. Ryter.	71
3. Infrared Polarimetry of Galactic Nuclei, by R.F. Knacke.	74
4. Infrared Emission from NGC 1068 by R.A. Dana and V. Petrosian.	77

## I. SOLAR SYSTEM OBJECTS

INFERENCE OF THE ATMOSPHERIC STRUCTURE OF JUPITER AND SATURN FROM THEIR  
FAR INFRARED SPECTRA

Th. Encrenaz and M. Combes - Groupe Planètes, Observatoire de Meudon

Recent improvements of infrared observations from airborne and balloon-borne experiments have opened the field of planetary spectroscopy in the far I.R. range ( $\lambda > 50\mu$ ). Furniss et al (1976) have obtained the first spectrum of Jupiter between 60 and 220 $\text{cm}^{-1}$ ; other spectra have been recorded in the same range from the NASA airborne I.R. observatory (C-141) by Erickson et al and Baluteau et al. No doubt that new far I.R. spectra of Jupiter and Saturn will be obtained soon from the Earth vicinity, and in the near future from space vehicles and probes.

The purpose of this paper is to evaluate the scientific return of such observations in the far I.R. spectral range, and to determine which spectral intervals are more promising to provide information about the vertical structure and composition of the atmospheres of Jupiter and Saturn.

Basic assumptions

At the present time, the vertical thermal structures of Jupiter and Saturn have been mainly obtained by the use of radiative transfer calculations; In the case of Jupiter, the thermal profile has also been derived from the inversion of infrared data. For Jupiter, we have chosen 2 models, corresponding respectively to these 2 different techniques. For Saturn, we have chosen a profile obtained from radiative transfer calculations, corresponding to an effective temperature of 90°K, this value of  $T_e$  giving the best general agreement between all the I.R. observations of Saturn.

In the far I.R. range, the expected observable components are  $\text{H}_2$  and  $\text{NH}_3$  on Jupiter,  $\text{H}_2$  on Saturn.  $\text{PH}_3$ , on Jupiter, is likely to be observable, as well as  $\text{CH}_4$  and  $\text{NH}_3$  on Saturn. In our calculations, we took into account  $\text{H}_2$ ,  $\text{NH}_3$  and  $\text{PH}_3$ . The  $\text{H}_2$  absorption is a function of  $\text{H}/\text{He}$ , through the pressure induced spectrum due to  $\text{H}-\text{H}_2$  and  $\text{H}_2-\text{He}$  collisions. We assumed  $\text{H}_2/\text{He}=5$ , in agreement with the solar value of  $\text{H}/\text{He}$ . The  $\text{NH}_3$  density distribution was assumed to be limited by its saturation law, with a solar  $\text{N}/\text{H}$  ratio below the clouds. Above the inversion level, the  $\text{NH}_3/\text{H}_2$  was assumed to be constant, in the lack of more information about this atmospheric region. However, on Jupiter, the  $\text{NH}_3/\text{H}_2$  ratio could be significantly reduced by photolysis above the inversion level; the effects of this process on the far I.R. jovian spectrum are taken into account below. In the case of  $\text{PH}_3$ , Prinn and Lewis have calculated a density distribution on Jupiter, based upon dynamical transfer processes, which are in agreement with the observation of  $\text{PH}_3$  on Jupiter at 5 and 10 $\mu$ .  $\text{PH}_3$  has been also tentatively observed on Saturn at 10 $\mu$ . We have assumed Prinn and Lewis' distribution on both Jupiter and Saturn. (Fig. 1)

Jupiter

The far I.R. spectrum of Jupiter (fig. 2) is dominated by the strong rotational spectrum of ammonia, showing a maximum absorption around 100 $\text{cm}^{-1}$  ( $J=4$ ). As a consequence it can be shown that the atmospheric layers where the far I.R. radiation comes from are close to the minimum of the temperature profile. Two important conclusions can be derived: (1) The continuous  $\text{H}_2$  absorption is hidden by the  $\text{NH}_3$  absorption in the whole far I.R. range, thus the  $\text{H}_2/\text{He}$  ratio cannot be inferred from measurements in this range; (2) The weight functions are expected to be wide because of the  $\text{NH}_3$  distribution which may decrease slowly above the convective zone. As a consequence, the observed radiance at a given frequency, should be dependent simultaneously upon the temperature minimum, the thermal lapse rate in the convective zone, and upon the temperature structure and  $\text{NH}_3$  distribution above the inversion level. Moreover, the  $\text{NH}_3$  density above this level may be strongly reduced by the effect of a possible photodissociation which remains unknown at present time. In conclusion, the spectral intervals where the influence of these different parameters can be separated, have to be carefully determined:

1) The absorption coefficient in the continuum at  $\lambda > 140\mu$  ( $J > 6$ ) is weaker than at 100 $\mu$ . Then, the radiation comes from the convective zone and there is no

contribution from the levels close to the minimum level. The only parameter able to modify the observed continuum is the  $T(P)$  relationship in the convective zone. Thus, under the assumption that  $\text{NH}_3$  follows its saturation law and that the thermal lapse rate is adiabatic, the  $T(P)$  profile in the convective zone can be obtained from the observation of the continuum at  $\nu > 140\text{cm}^{-1}$ . For the same reasons, the  $\text{NH}_3$  density in the convective zone may be obtained when the temperature profile is known from other spectral ranges.

2) The spectrum in the  $J \leq 5$  bands mainly depends upon the 2 to 4 atmospheric scale heights above the temperature minimum and thus, depends upon both the upper lapse rate and the efficiency of the  $\text{NH}_3$  photodissociation in this region. In particular, the cores of the  $J \leq 5$  bands are expected to be in emission if the  $\text{NH}_3$  photolysis is negligible and if the upper lapse rate is large. In contrast, if there is no emission at all, this implies that  $\text{NH}_3$  dissociation is important above the inversion level. In such a case, the value of the minimum temperature may be inferred from the observed brightness temperatures in the cores of the J-bands. But if the  $\text{NH}_3$  photodissociation appears to be negligible, it is impossible to derive more than an upper limit of the inversion temperature, which may exceed the actual minimum temperature by more than  $10^\circ\text{K}$  at  $0.5\text{cm}^{-1}$  resolution.

A special mention has to be made to the possible detection of  $\text{PH}_3$  in the far I.R. range. Calculations show that the  $\text{PH}_3$  lines are expected to be visible in absorption, until  $J=9$ , with a very small half-width. Thus, their observation will probably require a high resolution ( $0.1\text{cm}^{-1}$ ). In contrast with the  $5\mu$  observation, this  $\text{PH}_3$  measurement would have the interest of sounding the region of strong  $\text{PH}_3$  depletion.

The first far I.R. jovian spectrum has been obtained by Furniss et al (1976). The low frequency part ( $\nu < 125\text{cm}^{-1}$ ) strongly differs from our predictions; it may be significantly affected by residual pollution due to telluric  $\text{H}_2\text{O}$  lines. Above  $125\text{cm}^{-1}$ , the experimental spectrum is in reasonable agreement with atmospheric models in which the lapse rate is adiabatic in the convective zone, the minimum temperature around  $110^\circ\text{C}$  and the upper lapse rate positive. There is no need of under- nor supersaturation of  $\text{NH}_3$  to explain the observation.

### Saturn

The first characteristic of the far I.R. spectrum of Saturn concerns the observability of  $\text{NH}_3$ . Because of the low temperatures of Saturn's atmosphere, the  $\text{NH}_3$  cloud is expected to be very thick on Saturn, and the  $\text{NH}_3$  vapor much smaller than on Jupiter. Fig. 3 shows that the first multiplets of  $\text{NH}_3$  are likely to be observable on Saturn. From the observation of the  $\text{NH}_3$  absorption lines, it will be possible to test the validity of the  $\text{NH}_3$  saturation assumption on Saturn.

As a consequence of the low  $\text{NH}_3$  abundance on Saturn, it is shown from Fig. 3 that the far I.R. spectrum is dominated by the  $\text{H}_2\text{-H}_2$  and  $\text{H}_2\text{-He}$  absorption. This continuum can be observed everywhere from  $10$  to  $200\text{cm}^{-1}$ , apart from the individual absorption line due to any other minor constituent. Moreover the corresponding  $T_B$  show that the continuum radiation comes from the convective zone. Thus, it is possible to derive the  $T(P)$  profile in the convective zone from the observation of this continuum, and from this profile, an estimate of  $T_e$  can be derived, independent of the direct measurement of the integrated flux. Moreover, iterative methods as already used on Jupiter can give an estimate of the  $q = \text{H}_2/\text{He}$  ratio on Saturn. This is a major advantage of the far I.R. spectrum of Saturn: in the case of Jupiter, because of  $\text{NH}_3$ , we are limited to the  $16\text{-}40\mu$  range for the determination of  $q$  and the corresponding probed region is close to the minimum level, where the  $T(P)$  profile is only slightly function of  $q$ . In contrast, on Saturn, we have access to the convective zone where the dependence of  $T(P)$  upon  $q$  is more significant, although still smaller than its dependence on  $T_e$ .

The third major interest of the far I.R. spectrum<sup>e</sup> lays in the observability of  $\text{PH}_3$ . Fig 3 shows that the  $\text{PH}_3$  lines are clearly visible until  $J=9$ . Calculations show that it is possible to infer the  $\text{PH}_3$  distribution from the minimum  $T_B$  of the  $\text{PH}_3$  multiplets, on the basis of the  $T(P)$  profile derived from the continuum. The determination of the  $\text{PH}_3$  profile has a special astrophysical interest in the case of Saturn: it is not known yet whether strong dynamical processes could exist on Saturn or not. Thus, the

determination of the  $\text{PH}_3$  distribution on Saturn will be of primary interest in the study of the Saturnian dynamics.

#### Conclusion

The jovian far I.R. spectrum depends simultaneously upon many intricate parameters, and the vertical structure and composition of the jovian atmosphere cannot be derived unambiguously. Nevertheless, it would be of interest to measure  $T_g$  accurately ( $\Delta T \sim 2^\circ\text{K}$ ) in the continuum of the  $\text{NH}_3$  spectrum for  $J > 6$  ( $\sim 140\text{cm}^{-1}$ ), in order to infer the  $T(P)$  relationship in the convective zone. The investigation of the core of the  $J \leq 5$  bands at  $0.5\text{cm}^{-1}$  resolution will provide useful information about the lower stratosphere.

In contrast, the scientific return of the observation of Saturn in the far I.R. should be of highest interest. The  $T(P)$  profile below the minimum and the  $\text{H}_2/\text{He}$  ratio can be derived from this spectrum, at medium resolution ( $\sim 2\text{cm}^{-1}$ ), without additional assumptions. Moreover the  $\text{PH}_3$  distribution may be inferred from the minimum  $T_g$  of the  $\text{PH}_3$  multiplets, observable at medium spectral resolution ( $\sim 2\text{cm}^{-1}$ ).

ORIGINAL PAGE IS  
OF POOR QUALITY

Fig. 1

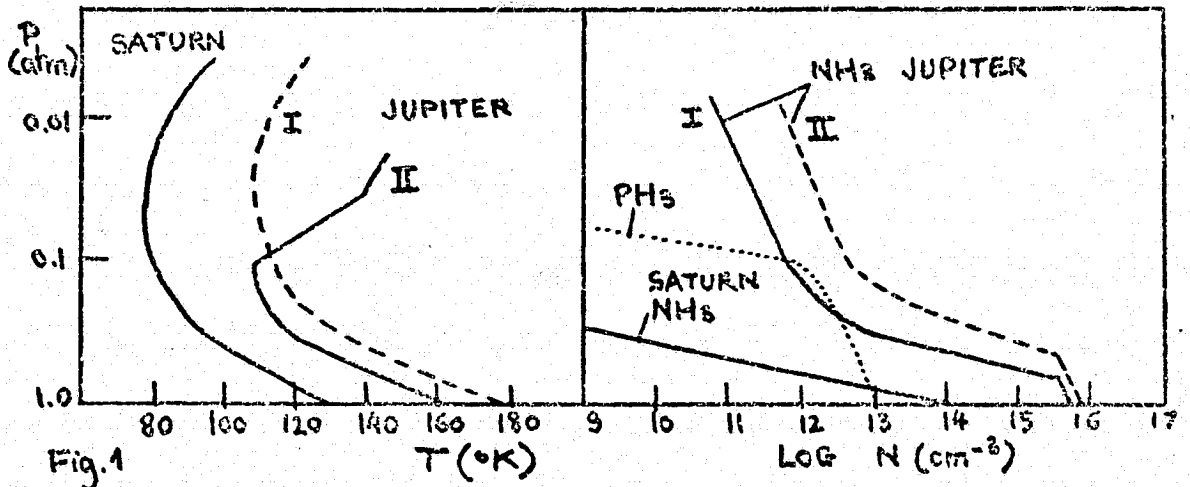


Fig. 1

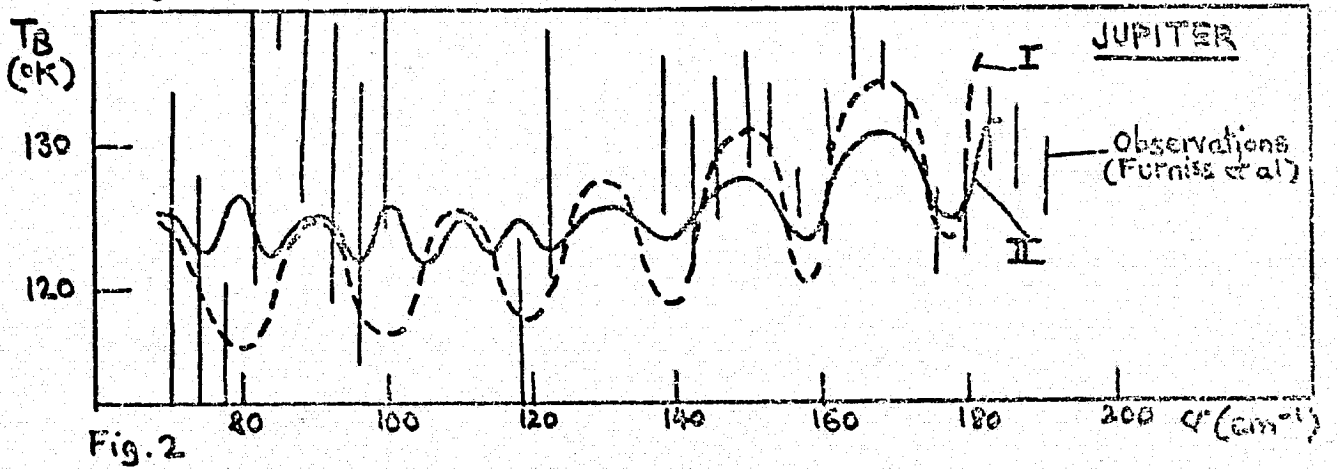


Fig. 2

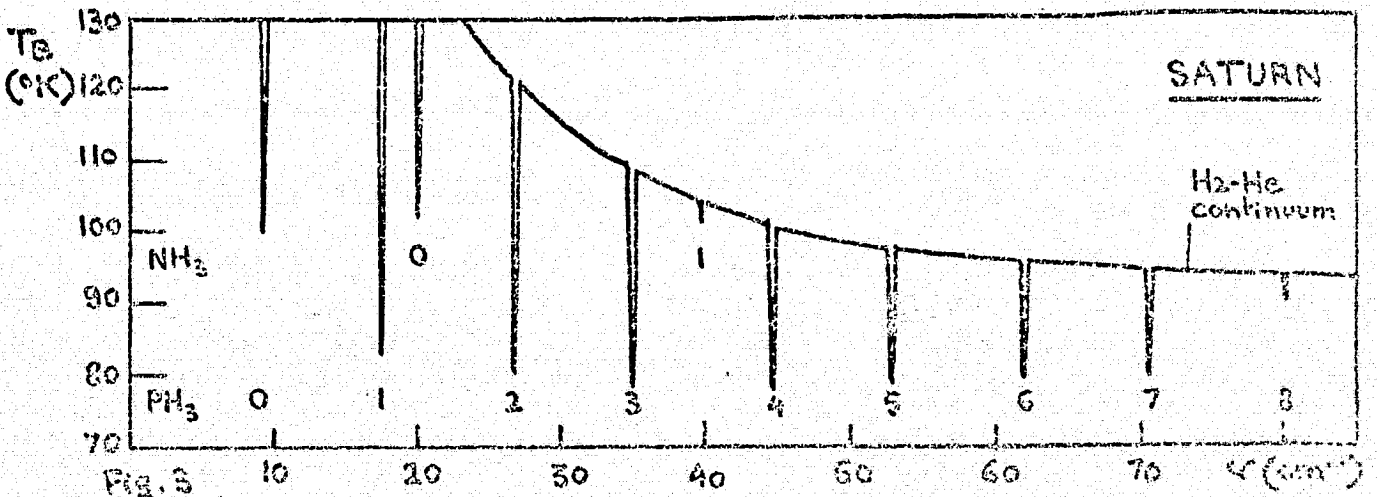


Fig. 3

## Abstract

## Far Infrared Spectrophotometry of the Giant Planets

by

E.F. Erickson, D. Goorvitch, J.P. Simpson, and D.W. Strecker  
Astrophysical Experiments Branch  
NASA-Ames Research Center, Moffett Field, CA 94035

A fundamental problem of infrared astrophysics is the thermal emission of Saturn and Jupiter. Airborne photometry by Aumann, Gillespie, and Low (Astrophys. J. 157, 169 (1969), and by Armstrong, Harper, and Low (Astrophys. J. 178, L89 (1972)) gave a value for the ratio  $R$  of the power emitted to the power absorbed by Jupiter of  $R=2.5\pm 0.5$ . Observations from Pioneer 11 (Ingersoll et al., Science 188, 472 (1975)) gave a value of  $R=1.9\pm 0.2$ . In the case of Saturn, the observational problem is complicated by the presence of the rings, which contribute a thermal flux comparable to that from the disc (Nolt et al., ICARUS, in press; Rieke, ICARUS 26, 37 (1975)). Theoretically, internal power sources in the giant planets could exist due to gravitational contraction or cooling of the primordial material (Pollack et al., ICARUS (1977) in press). Shapes of the thermal spectra depend extensively on details of the planetary atmospheres (Orton, ICARUS 26, 125 (1975); Caldwell, ICARUS, (1977) in press).

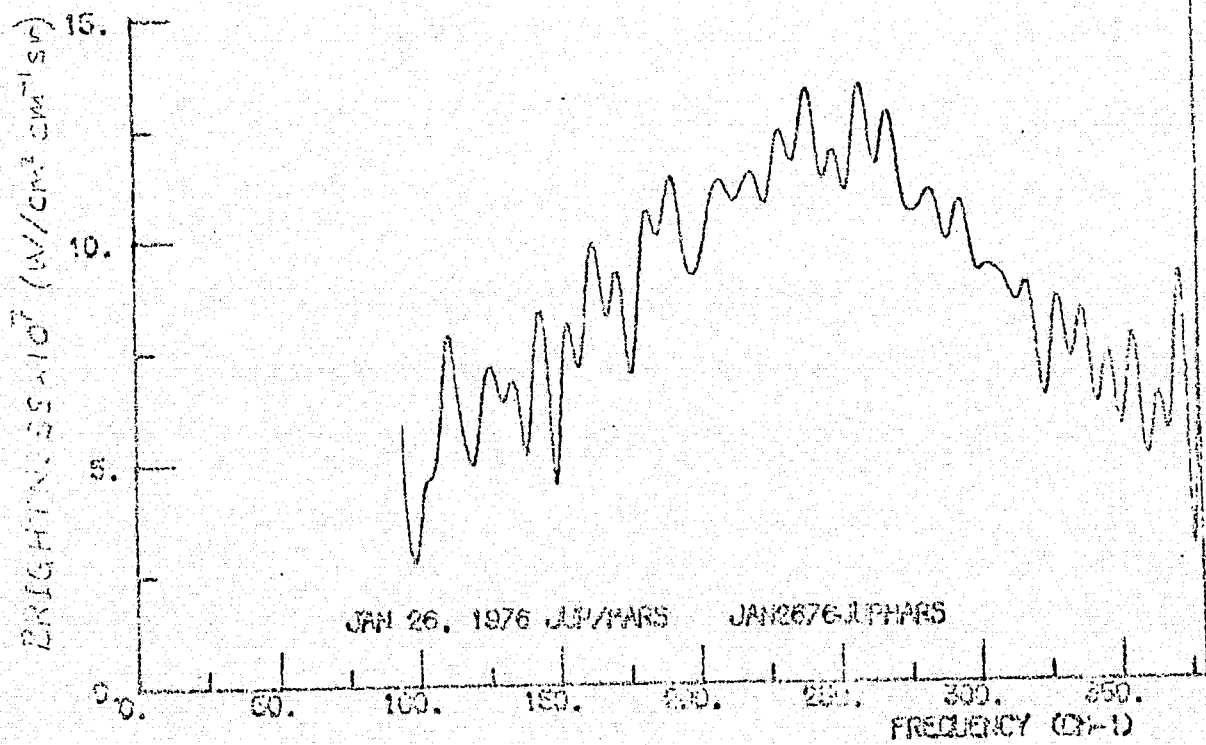
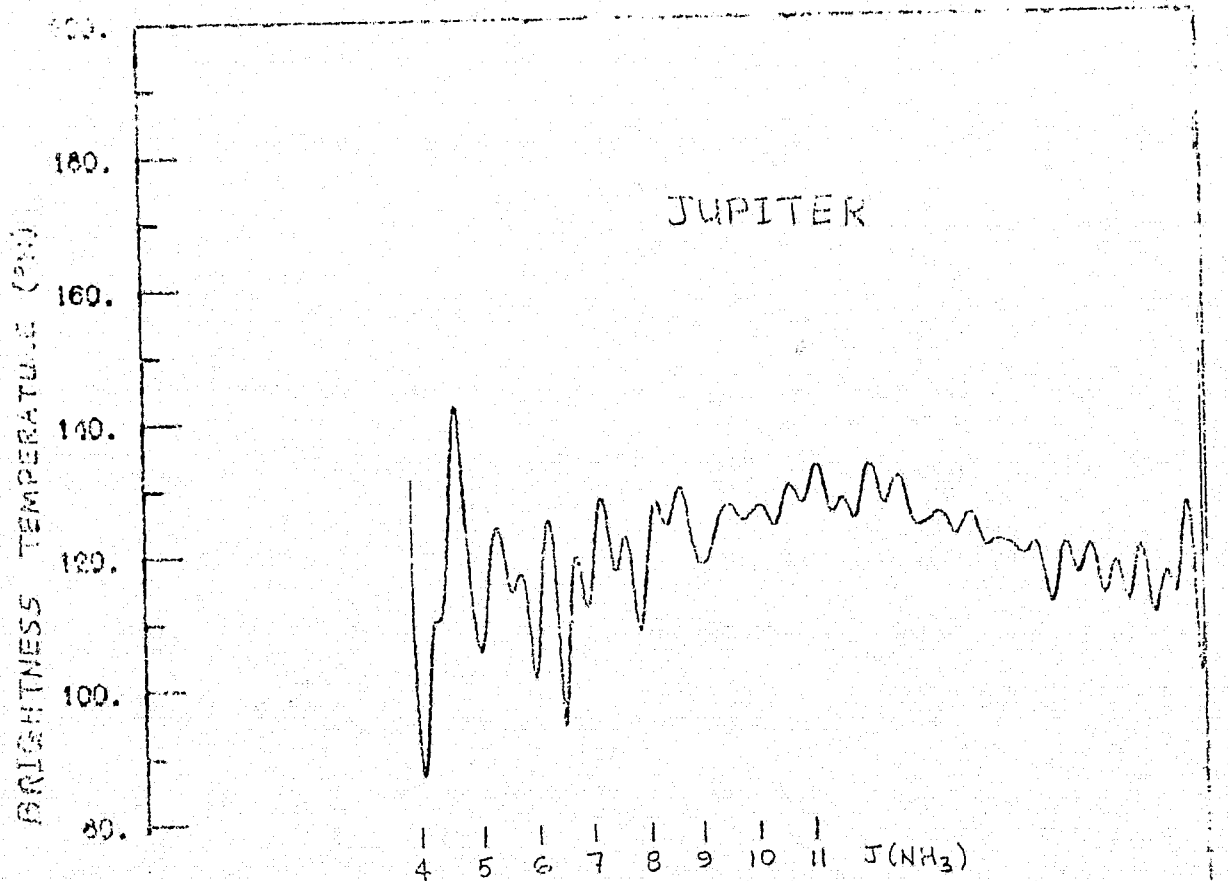
A second important consideration is the use of the planets as calibration sources for far infrared observations. Mars is a relatively good calibration source because the tenuous character of its atmosphere simplifies its thermal emission, although there is some uncertainty in the spectrum due to uncertainty in the emissivity of the surface (Wright, Ap. J. (1976) in press), and weather conditions. However, Mars is often inaccessible to infrared observers, and it is frequently more convenient to use one of the giant planets for calibration.

We observed Mars, Jupiter, and Saturn on each of four flights of the G.P. Kuiper Airborne Observatory using a Michelson interferometer in early 1976. On January 20 and 26 spectra were obtained from 90-370  $\text{cm}^{-1}$ , and on February 3 and 4 spectra were obtained from 100-430  $\text{cm}^{-1}$ . In this paper we discuss the analysis of these data at low resolution ( $\sim 7 \text{ cm}^{-1}$ ), to obtain the brightnesses of Jupiter and Saturn in the vicinity of their thermal emission maxima. The measured spectra of Jupiter and Saturn were divided by the measured spectrum of Mars to cancel the instrument response function, and to first order, absorption by telluric  $\text{H}_2\text{O}$ . We corrected the resulting ratios for loss of energy due to diffraction in the telescope aperture, using the 72" FWHM aperture profile measured on Mars. Multiplying these ratios by the appropriate solid angle ratios for the planets and the brightness of Mars as obtained from the model of Wright (op cit) gave the brightness for Jupiter and Saturn. The results of this analysis for the Jupiter data of January 26 are shown in the accompanying figure.

It is clear from the figure that the instrument bandpass (90-360  $\text{cm}^{-1}$  FWHM) brackets the thermal emission maximum well. Most of the features are due to  $\text{NH}_3$  rotational bands in the Jovian atmosphere, incompletely cancelled

telluric  $H_2O$  absorptions, and noise in the measurement. The frequencies of the  $NH_3$  features are indicated by the values of the corresponding rotational quantum number,  $J$ . Integrating the brightness function to obtain the total flux, we find the ratio of power emitted from 70 to  $370\text{ cm}^{-1}$  to power absorbed from the sun to be  $R=1.02$ , assuming an albedo of 0.45. The data from January 21 give  $R=1.06$ . It is clear that the major uncertainty in this result is due to the Mars model used to calibrate these data. We emphasize that our value for  $R$  includes most, but not all, of the thermal radiation emitted by Jupiter. A 130K blackbody emits 40% of its power outside our bandpass.

In the paper presented at the meeting, our Jupiter data will be compared with those of other observers and the theory of Orton (op cit); the significance of our value of  $R$  will be discussed. Our data on Saturn will be compared with the theory of Caldwell (op cit).



ORIGINAL PAGE IS  
OF POOR QUALITY

FUNDAMENTALS OF  $\text{PH}_3$  AND  $\text{NH}_3$  IN THE INFRARED:  
CURRENT PURSUITS IN LABORATORY SPECTROSCOPY

K. Narahari Rao  
Department of Physics  
The Ohio State University  
Columbus, Ohio 43210

With the availability of newer<sup>1,2</sup> planetary spectra revealing the presence of phosphine ( $\text{PH}_3$ ) as a constituent in the atmosphere of Jupiter, it has been considered important to examine the laboratory data in the infrared for this molecular species. A brief discussion will be given of the spectra of both the  $\text{PH}_3$  and  $\text{NH}_3$  molecules with reference to a few specific spectral regions where measurements which are not yet available in the open literature exist. The data have been obtained by employing vacuum grating spectrographs with a resolution of about  $0.02 \text{ cm}^{-1}$  in the near infrared where the  $\nu_1$  and  $\nu_3$  bands are observed and about  $0.05 \text{ cm}^{-1}$  at the longer wavelengths where the  $\nu_2$  and  $\nu_4$  bands occur.

Ammonia (a)

Extensive scans have been made in the  $3091\text{-}3591 \text{ cm}^{-1}$  region where the major contribution to absorption is due to the  $\nu_1$  and  $\nu_3$  fundamentals. The  $\nu_2$  and  $\nu_4$  bands, respectively, located at  $770\text{-}1280 \text{ cm}^{-1}$  and  $1420\text{-}1860 \text{ cm}^{-1}$  have also been studied extending the original investigation by Nielsen, Garing, and Rao.<sup>3</sup>

---

(a) John Curtis and David Stout participated.

The availability of these data combined with the submillimeter-wave studies made in USSR<sup>4</sup> by using acoustic detection, prompted Papousek and his coworkers, at Prague<sup>5</sup>, to embark on a more sophisticated theoretical model which is expected to lead to an improved set of molecular parameters for ammonia.

### Phosphine

Maki, Sams, and Olson<sup>6</sup> and Yin and Rao<sup>7</sup> have recently studied a few of the infrared bands of this molecule using high resolution spectrometers. The present experiments in the laboratory<sup>(b)</sup> are confined to a careful high resolution study of the  $\nu_1$  and  $\nu_3$  band region which is of particular interest to the Jupiter spectrum and which has not been recently studied using the present day technology. At the time of writing this abstract, observations are still continuing and several interesting details have already emerged. A summary of this work will be presented.

A few comments will be directed to the development of a newer version of the Mulliken report<sup>8</sup> to take account of modern research in molecular spectroscopy.

---

<sup>(b)</sup>Da-Wun Chen, David Applebaum, and William Ivancic, are participating in this research.

## REFERENCES

1. S. T. Ridgway, B.A.A.S. 6, 376 (1974).
2. Harold Larson, University of Arizona, and R. Beer, JPL (Private Communication).
3. H. H. Nielsen, J. S. Garing, and K. Narahari Rao, J. Mol. Spectrosc. 3, 496 (1959).
4. A. F. Krupnov and A. V. Burenin, Chapter 2 in Molecular Spectroscopy: Modern Research, Vol. II, Ed. K. Narahari Rao, Academic Press (1976).
5. See, V. Spirko, J.M.R. Stone, and D. Papousek, J. Mol. Spectrosc. 60, 159 (1976). Further work is in progress and the results will be made available in due course.
6. A. G. Maki, R. L. Sams, and W. B. Olson, J. Chem. Phys. 58, 4502 (1973).
7. P.K.L. Yin and K. Narahari Rao, J. Mol. Spectrosc. 51, 199 (1974)
8. R. S. Mulliken, J. Chem. Phys. 23, 1997 (1955).

PRELIMINARY MEASUREMENTS OF THE EMISSION SPECTRUM  
OF THE ZODIACAL CLOUD

D. A. Briotta\* and J. R. Houck

Center for Radiophysics and Space Research  
Cornell University  
Ithaca, N.Y. 14853

A Helium-cooled spectrometer was used to measure the emission spectrum of the zodiacal dust cloud in the 8-14 $\mu$  band ( $\Delta\lambda \approx 0.4\mu$ ). The spectrometer used a 16 element SiAs array. It was fed by an f/3, 17 cm Helium-cooled Cassagrain telescope carried to a peak altitude of 266 km on 14 October 1975 by an Astrobee F sounding rocket. The attitude control system was programmed to scan the field of view back and forth across the ecliptic plane while slowly scanning in ecliptic longitude from an elongation angle of 80° to 135°. The peak to peak amplitude of the resulting triangle wave pattern was 60°. Despite problems with the launch vehicle a successful scan across the ecliptic plane was completed at an elongation angle of 104°.

The resultant spectrum has a peak amplitude of  $7.5 \times 10^{-11}$  w/cm<sup>2</sup> sr/ $\mu$  at a wavelength of 9.5 $\mu$ . The spectrum can be fit by a two-component model. The major component consists of small silicate grains ( $\alpha = 6.5 + 2.8\mu$ ,  $T = 374 + 25^\circ\text{K}$ , dilution =  $2.4 + 0.8 \times 10^{-8}$ ) and a blackbody component ( $T = 284 + 71^\circ\text{K}$ , dilution =  $2.1 + 1.7 \times 10^{-8}$ ). For the purpose of this fit the silicate material is assumed to have the same optical properties as the particles responsible for the 10 $\mu$  emission feature associated with the Trapezium infrared source. The blackbody component may be due to scattered earth light reaching the detectors. These results are discussed in the context of current zodiacal light and particle collection studies.

This work was supported by AFGL contract F 19628-73-C-0242.

\*Permanent address: Department of Physics and Astronomy,  
University of Wyoming, Laramie, Wyoming 82070

## II. STELLAR SOURCES

THE EFFECTS OF WINDS AND CORONAS OF HOT STARS  
ON THE INFRARED AND RADIO CONTINUA

by

Joseph P. Cassinelli and Lee Hartmann

Washburn Observatory  
University of Wisconsin-Madison  
Madison, Wisconsin 53706

Abstract

The theory of the formation of infrared and radio continua is extended to include the effects of steep temperature gradients and coronas. The presence of high temperature zones in the winds from hot stars has been suggested by recent Copernicus satellite observations. We consider models in which the temperature is large only over a small range in radius. The density in the winds of hot stars is high enough for recombination to cool the flow where mechanical energy deposition ceases. Excess radiation at long wavelengths arises in the winds because of the  $\lambda^2$  dependence of free-free opacity. We find the coronal region causes a broad bump in the infrared continuum at about 20-100 $\mu$ , with a maximum excess of almost 2 magnitudes. Variations of the distribution of density with height can also cause turnover in the continuous energy distribution, however only temperature decreases, as occurs in the recombination region, can cause spectral gradients much steeper than the Rayleigh-Jeans gradient.

*Spectrophotometry of Early-Type Stars from 1.2 to 4.2 Microns*

*Jeffrey D. Scargle*  
*Theoretical and Planetary Studies Branch*

*F.C. Witteborn, D.W. Strecker, and E.F. Erickson*  
*Astrophysical Experiments Branch*

*NASA-Ames Research Center*

*In the infrared many early-type stars show an excess of radiation over that expected from the photosphere of the star. In almost every case the existence of an IR excess is coupled with the presence of emission lines in the visible part of the spectrum. The IR continuum and the emission lines are both presumed to arise in an extended shell of gas and possibly dust which surrounds the star. The mechanism for the IR excess may be free-free emission (proton-electron,  $H^-$ , or  $H_2^-$ ) by the hot ionized gas, thermal emission by dust, a combination of the two, or some other mechanism entirely.*

*In order to elucidate the nature of these IR excesses a number of early-type stars have been observed with the 91 cm. telescope on the Kuiper Airborne Observatory, using a cooled filter wedge spectrometer giving about 2% spectral resolution in the range 1.2 to 4.2 microns. The primary goal of this program is to obtain accurately calibrated spectra of infrared-excess and normal early-type stars. The stellar contribution to the IR excess stars can then be subtracted to yield the shell spectrum, which can then be compared to models for the emission process. In addition, emission lines from the shell can be studied, although it must be remembered that at this resolution P-Cygni profiles will be severely washed out.*

*The spectra of the stars gamma Cassiopeiae, P Cygni, beta Lyrae, zeta Ophiuchi, and XX Ophiuchi (as well as the normal A0V star alpha Lyrae) were measured during the June, 1976 flight series. Absolute calibration was based on the data for alpha Lyrae and the model atmosphere for this type star by Mihalas. The flux expected from the photosphere was estimated by assuming zero shell contribution at the V-magnitude bandpass (0.55 micron) and using a model atmosphere appropriate to the spectral type of the star in question. The results of this procedure will be shown and compared to models of the IR excess. In several of the stars the alpha and beta lines of the Paschen and Brackett series of hydrogen are seen in emission. In P Cygni, and possibly also zeta Ophiuchi, an absorption feature appears at 3.41 microns, and is so far unidentified.*

0.85 to 2.5 Micron Spectrum of  $\gamma$  Cassiopeia

M. F. Campbell and R. I. Thompson, Steward Observatory, University of Arizona

A spectrum of the B0IVe star  $\gamma$  Cassiopeia taken on 1976 October 5 with the Steward Observatory Fourier transform spectrometer at the Cassegrain focus of Steward's 2.3 meter telescope is presented. The spectrum extends from 4000 to 12000  $\text{cm}^{-1}$  at a resolution of 2  $\text{cm}^{-1}$ . Similar spectra have been obtained by Larson, Trefers, and Fink and by Maillard.

The optical spectrum of  $\gamma$  Cas shows a number of variable emission lines, principally of hydrogen. The emission lines often show a central absorption, and the shape is variable as well as the strength. There is also an infrared excess relative to a normal B0 star. The infrared excess and the emission lines are thought to originate in an extended atmosphere. The atmosphere, or shell, is believed to be massive because of the existence of absorption lines not associated with the B star, but with cooler material.

The present spectrogram shows emission lines of hydrogen from Paschen  $\beta$  through P18, Brackett  $\gamma$  through B20, and of helium at 1.0830 and 2.0581  $\mu$ . Within the Brackett and Paschen series, the lines are of approximately equal strength, not showing the decrement expected from applying recombination theory to an optically thin gas cloud. The hydrogen emission lines are structured, showing extension on the blue side.

Comparison with an independent spectrum of the A0 star  $\alpha$  Lyra shows that  $\gamma$  Cas has an infrared excess over the expected stellar continuum.

The emission line spectrum is studied by assuming the existence of an extended atmosphere or shell and applying recombination theory. The resultant physical parameters are then used to derive the continuum emission of the shell.

Aircraft and Ground Based Infrared Spectroscopy of MWC 349, MWC 297 and Lk H $\alpha$  101 - Rodger I. Thompson, Steward Observatory, U of Arizona, Edwin F. Erickson, D. W. Strecker and Fred C. Witteborn, NASA Ames Research Center -  
I. Introduction

A co-operative program of combined aircraft and ground based infrared spectroscopy of young stellar objects is being carried out in order to determine the physical conditions present in the newly formed stars. A selection criterion of highly reddened emission line objects with strong infrared excesses has been used in selecting the objects for study. Three such objects (MWC 349, MWC 297, and Lk H $\alpha$  101) are discussed in this abstract. These objects are concluded to be newly formed luminous O or B stars that are in the process of blowing out by radiation pressure the material from which they were formed. At a slightly earlier epoch these stars were completely encased in their natal dust cocoons and only detectable by thermal dust remission. These stars have therefore just been unveiled and represent the earliest stage at which a star can be directly observed.

II. Observations

A continuously variable filter wheel spectrometer at the bent cassegrain focus of the NASA C-141 Gerard P. Hinper Observatory was used to obtain high altitude spectra between 1 and 4 microns. These spectra which are essentially free of telluric water vapor absorption have a resolution of  $\Delta\lambda/\lambda \sim 0.02$ . Spectra of MWC 349 and MWC 297 were taken during a flight on June 10, 1976 and the Lk H $\alpha$  101 spectrum was obtained in a flight in January 1976.

On June 10, 1976 ground based spectra of MWC 349 and MWC 297 were taken with the Steward Fourier transform spectrometer at the cassegrain focus of the Steward Observatory 2.3 meter telescope between 1 and 2.5 microns. These spectra taken concurrently with the aircraft spectra have a resolution of  $\Delta\kappa = 2\text{cm}^{-1}$  over the spectral range from  $4000\text{ cm}^{-1}$  to  $10,000\text{ cm}^{-1}$ . Concurrent spectra were taken as there is some evidence (Greenstein 1973) that the line emission strength in MWC 349 may vary significantly in less than 24 hours. Subsequent ground based spectra at the same resolutions were taken of MWC 349 and Lk H $\alpha$  101 in September 1976 with an extended wavelength range of  $0.85\mu$  to  $2.5\mu$ .

The infrared spectra of these objects are dominated by strong emission lines of the hydrogen Brackett and Paschen series superimposed on a red continuum. The aircraft spectra of all three objects show strong emission in Paschen  $\alpha$  which is unobservable from the ground because of telluric water vapor absorption. Brackett  $\alpha$  emission is also observed in MWC 349 and MWC 297. Brackett  $\alpha$  was not in the spectral range of the filter wheel used in the January Lk H $\alpha$  101 observations.

The ground based spectra show the Brackett  $\alpha$  and Brackett 10-20 lines as well as  $P_{\beta}$ ,  $P_{\alpha}$  and OI  $\lambda$   $1.1287\mu$  in emission in all of the objects. He I emission lines are present in MWC 349 including He I 10830 and He I 20581 which will be discussed below. The extended wavelength range of the September MWC 349 includes higher order Paschen emission lines including  $P_{\delta}$ . Both Lk H $\alpha$  101 and MWC 349 display a strong emission line at  $5925\text{ cm}^{-1}$  which corresponds to an OI quintet line from a highly excited level. There also exist in the spectra of MWC 349 and Lk H $\alpha$  101 several unidentified emission lines.

III. Analysis

MWC 349 has the most extensive quantitative observational material of the three objects and will be analyzed in the following with reference made to the other objects. To begin the analysis it is assumed that the line radiation

arises from recombination in an H II region surrounding the hot central star. The observed relative strengths of  $B\alpha$  and  $P\delta$  which have the same upper level then yield a value for the reddening of  $2.1 \pm 0.1$  mag between  $4617 \text{ cm}^{-1}$  and  $9951 \text{ cm}^{-1}$ . Scaling of Johnson's (1968) extinction curve for Cygnus then yields the extinction at all other wavelengths. Application of the derived extinction to the calculated emission line spectrum yields agreement to within 15% for all of the observed Brackett and Paschen lines as well as for the  $H\alpha$  and  $H\beta$  line strengths taken from Kuhl's (1973) optical data. The only discordant line is  $H\alpha$  for which Kuhl's (1973) data gives a value  $\sim 50\%$  below the predicted value. The weakness of the  $H\alpha$  line may contribute to this discrepancy.

If a distance of 3kpc is assumed then the value of  $\text{Ne}^{2+}$  can be calculated for the nebula. This value from  $B\alpha$  and  $H\beta$  yields  $\text{Ne}^{2+} = 3 \pm 0.3 \times 10^{61} \text{ cm}^3$ . The Zanstran temperature implied by this measurement is on the order of  $35,000^\circ\text{K}$ .

The Zanstran method is appropriate only in the H II region is ionization bounded. The presence of strong He I 20581Å emission implies that it is since a high optical depth in the resonance He I transition at 584Å is needed. This transition strength for normal H/He ratio is less than that for  $\text{Ly}\alpha$ ; thus the nebula is ionization bounded.

The strength of the OI 1.1287 $\mu$  line proves that  $\text{Ly}\beta$  fluorescence is the source of the strong OI 8446 line at near infrared data. Comparison of the OI 1.1287 $\mu$  line with the OI 8446 line is unpublished scanner data by Grandi (1976) indicates that the number of photons emitted by the two lines are equal whereas the photon flux from other feed lines to OI 8446 is significantly less. OI 8446 emission therefore occurs via  $\text{L}\beta$  pumping to the upper state of OI 1.1287 $\mu$ . At present the excitation of the OI 5925  $\text{cm}^{-1}$  line is not understood therefore its identification must still be considered tentative.

Kuhl's analysis of the continuum reddening of MWC 349 yields a higher value for the extinction at V by about 1.4 mag. The excess continuum reddening increases toward shorter wavelengths and is consistent with earlier results (Thompson and Reed 1976) which implied that the infrared emitting dust was interior to the H II region. Radio measurements of the extent of the H II region yielded a size on the order of  $10^{-2}$  pc whereas the dust temperature required that the dust be at a distance of  $10^{-4}$  pc. The circumstellar dust must be irregularly distributed therefore to allow ultraviolet photons to escape and produce the surrounding H II region. A similar geometry is also postulated for Lk H $\alpha$  101.

#### IV. Conclusions

All of the above analysis indicates that the observed objects are young luminous objects with line radiation coming from a surrounding H II region. The extinction and infrared emission comes from surrounding dust which is part of the natal protostellar cloud of the star. The radiation from the star has disrupted the cloud into a clumpy distribution of dust and gas.

#### References

- Grandi, S. 1976, Private Communications.  
 Greenstein, J. L. 1973, Ap. J. (Letters), 184, L23.  
 Johnson, H. L. 1968 in "Nebulae and Interstellar Matter" Edited by Middlehurst, B. M. and Aller, L. H., The University of Chicago Press.  
 Kuhl, L. V., 1973, Ap. Letters, 14, 141.  
 Thompson, R. I., and Reed M. A., 1976, Ap. J. (Letters), 205, L159.

Abstract of paper for the symposium on Recent Results in Infrared  
Astrophysics January 12-14, 1977 at NASA-Ames

Title: Spectral Observations of Eta Carina at 4-Microns

Authors: David K. Aitken, Barbara Jones (University College London)  
J.D. Bregman, D.F. Lester, D.M. Rank (Lick Observatory)

Abstract:

The spectrum of the Eta Carina nebula has been measured in the vicinity of 4-microns with a resolution of 0.025-microns. The spatial distribution of the thermal continuum and Brackett $\alpha$  ( $n=5-4$ ) line at 4.05-microns was traced across the nebula.

The central core of the nebula is marginally resolved with a full width at half maximum of 2.6-arcsec. The Brackett $\alpha$  and 4-micron continuum profiles are roughly exponential and decrease proportionally out to approximately 8-arcsec from the center where the continuum falls below our detection limit. There is some indication that the line radiation persists out to 15-arcsec. Comparison of the 4-micron and 10-micron continuum profiles shows a decrease in the dust temperature of at least several hundred degrees from the center to the edge of the nebula.

The hydrogen line measurements yield an essentially extinction free value of the emission measure of the source. An ionized core density of  $10^6 \text{ cm}^{-3}$  is derived, and a central source intensity of about  $10^{50} \text{ sec}^{-1}$  of Lyman continuum photons is required to maintain the HII region. This is comparable to the integrated luminosity of the object. The source of the ionizing radiation must be very hot, perhaps an early type O star. Comparison of the Brackett $\alpha$  strength with H $\gamma$  suggests a visual extinction of  $3.8^m$  to the source.

Airborne Photometric Observations between 1.25 and 3.25  $\mu$  of late-type stars

by

G. C. Augason

NASA-Ames Research Center, Moffett Field, CA 94035

H. L. Nordh

and

S. G. Olofsson

Stockholms Observatorium, S-133 00 Saltsjöbaden, Sweden

Abstract

During seven flights in April/May 1976 with NASA's Lear Jet aircraft, equipped with a gyro-stabilized 30 cm telescope and a liquid nitrogen cooled PbS detector, the stars  $\alpha$  Boo (K2 III p),  $\alpha$  Sco (M1 - M2 Iab),  $\mu$  Gem (M3 III) and  $\alpha$  Her (M5 II) were observed in five photometric bands between 1.25  $\mu$  and 3.25  $\mu$ . The details of the filter system are given in Table 1. The atmospheric extinction in each filter has been calculated on the basis of a simple atmosphere model (Augason et al., 1975). Noteworthy is that at the operating altitude of the Lear Jet ( $\sim 14$  km) the transmission is essentially 100% at these short infrared wavelengths. In the last column the basic objective of each filter is indicated.

Table 1

Filter	$\lambda_c(\mu)$	$\Delta\lambda(\mu)$	% Atmos. Trans. within band-pass	Comment
F 1	1.27	0.17	99.8	Continuum
F 2	1.49	0.19	99.3	CN( $\Delta v = -1$ )
F 3	1.75	0.31	99.1	Continuum
F 4	2.40	0.17	99.9	CO( $\Delta v = +2$ )
F 5	3.25	0.45	99.7	Continuum

The purpose of the program was to provide data for detailed comparisons with stellar model atmospheres and to serve as guidelines for further observations. To this end airborne observations are advantageous for two reasons: (1) the transmission profiles of the photometric bandpasses are not affected by absorption in the earth's atmosphere, and (2) total absorptions or band strengths of otherwise heavily obscured molecules or radicals like CN and CO can be obtained. Although these two species can be studied at high spectral resolution from the ground, it is difficult that way to obtain a quantitative measure of the total amount of light that they absorb in the stellar atmosphere.

Before the flight series the response of the photometer was determined in the laboratory by measuring a well stabilized block-body source, operated at two different temperatures, 1000 K and 1300 K, respectively. Since the telescope was flown open port, since the atmospheric extinction was essentially zero, and since the reflectance of the aluminum coated telescope mirrors is practically constant in the interval 1-4  $\mu$ , the response measured in the laboratory should hold also in flight.

In Fig. 1 we have plotted the observed relative intensities, normalized at  $1.27 \mu$ , relative to  $\alpha$  Boo. In view of column four in Table 1, no extinction corrections have been applied. Since  $\alpha$  Aur and  $\alpha$  Sco were both measured on just one night, the corresponding curves should be used with some caution. For the stars measured during more than one night, the mean errors in the relative intensities range from  $\pm 1\%$  to  $\pm 9\%$  with an average mean error of  $\sim \pm 3\%$ . The reduction of the blackbody measurements is not yet finished, so the flux-curves will not be discussed here.

Since the energy distributions of late-type stars vary strongly with wavelength it is difficult to extract information from a diagram like that in Fig. 1 but some comments can readily be made. Comparison with model atmospheres are presently being made and the results will be published elsewhere.

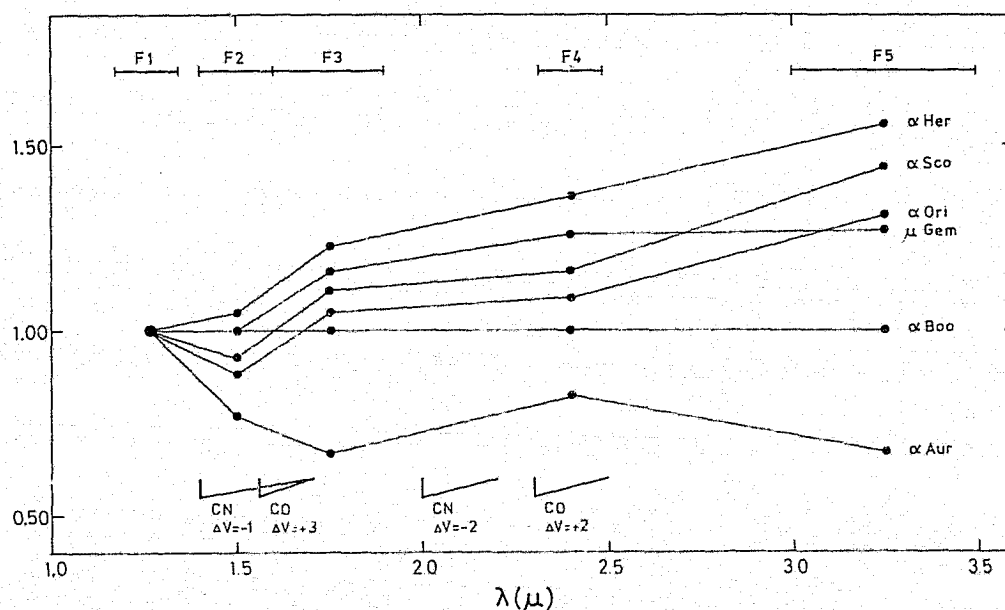


Fig. 1 Relative intensities, normalized at  $1.27 \mu$ , are plotted relative to  $\alpha$  Boo. The filter positions and widths are indicated at the top of the figure. At the bottom of the figure the position and shape of the pertinent CN and CO absorptions are sketched.

#### $\alpha$ Aur

Provided the observations are correct, the flux seems to be surprisingly low in the filters F2 and F3. Whether this "anomaly" could be due to the fact that  $\alpha$  Aur is a spectroscopic binary (G5 III + G0 III, see Wright, 1954) and has been reported as an X-ray source (Catura *et al.*, 1975) merits further study.

#### $\alpha$ Ori and $\alpha$ Sco

It is immediately seen that the absorption from both CN and CO is much stronger in these stars than it is in  $\alpha$  Boo, in agreement with what one would expect from the known temperature and luminosity sensitivity of these molecules. A tendency for  $\alpha$  Sco to be slightly redder than  $\alpha$  Ori is also seen.

$\mu$  Gem

The most remarkable thing is the very low flux in filter F5. (The observations of both  $\alpha$  Boo and  $\mu$  Gem are good enough to make the position of this point accurate to within  $\pm 5\%$ ). We have at present no good explanation to offer for this and we suggest that more observations be made longward of  $3 \mu$ .

 $\alpha$  Her

No spectacular features other than the redness can be attributed to this star on the basis of Fig. 1 and without a quantitative analysis based on an appropriate model atmosphere.

Acknowledgements

We would like to thank the staff of the Lear Jet aircraft for their great efforts. Drs. L. J. Caroff, E. F. Erickson, and F. C. Witteborn participated as observers on some flights, which is gratefully acknowledged. Two of us (L.N. and G.O.) were generously supported by the Swedish Board for Space Activities through Grant DR 1148.

References

- Augason, G. C., Mord, A. J., Witteborn, F. C., Erickson, E. F., Swift, C. D., Caroff, L. J., and Kunz, L. W., 1975, Appl. Opt., 14, 2146.
- Catura, R. C., Acton, L. W., and Johnson, H. M., 1975, Astrophys. J. (Letters), 196, L 47.
- Wright, K. O., 1954, Astrophys. J. 119, 471.

INFRARED NARROW BAND SPECTROPHOTOMETRY OF MOLECULAR BANDS IN LATE TYPE STARS

CURTIS P. RINSLAND AND ROBERT F. WING

Ohio State University, Columbus, Ohio

RICHARD R. JOYCE

Kitt Peak National Observatory, Tucson, Arizona

I. INTRODUCTION

Recent observations of <sup>12</sup>C/<sup>13</sup>C ratios in G, K, and M giant stars (c.f. Lambert and Tomkin 1974; Lambert, Dearborn, and Sneden 1974) have made it increasingly evident that many "normal" oxygen-rich giant stars have undergone a significant degree of mixing of surface material with interior material that has been processed by nuclear reactions. In order to study the effects of chemical processing on the atmospheres of red giant stars we have developed a new narrow band system for spectrophotometry of molecular bands in the near infrared (1.5-4.1μ) region. The bandpasses for this program have been selected by examining high resolution FTS data obtained using the 5-m Palomar telescope (Connes and Michel 1974) and the 4-m Kitt Peak telescope (Ridgway 1976). Molecules containing the light elements H, C, N, and O and their detectable isotopes will be studied in G, K, and M stars. These elements are of critical importance in understanding the type and amount of nuclear-processed material which has reached the surfaces of late type giant and supergiant stars.

This abstract will provide a discussion of the selection of the bandpasses for the program and a description of the methods to be employed in interpreting the data. The first observations on this system were obtained during September and October 1976 at Kitt Peak National Observatory.

II. SELECTION OF THE BANDPASSES

The abundant elements H, C, N, and O provide several molecules with detectable vibration-rotation or electronic transitions in the near infrared region. We have chosen to observe the molecules <sup>12</sup>CO, <sup>13</sup>CO, CN, OH, SiO, H<sub>2</sub>O, and C<sub>2</sub> within three atmospheric windows between 1.5 and 4.1μ. Bandpasses for the program are listed in Table I.

H BAND REGION (1.5-1.75μ). The molecules OH, CN, CO, C<sub>2</sub>, and H<sub>2</sub>O all have transitions in this spectral region. Also many atomic lines occur.

The Δv=2 sequence of the vibration-rotation bands of OH increase rapidly in strength to later spectral types. Although the (2,0) and (3,1) R branch heads are not observable from the ground, the (4,2), (5,3), and (6,4) bandheads can be detected as well as many strong P branch lines. We have chosen to measure the (4,2) head at 6505 cm<sup>-1</sup>. It occurs beyond the Δv=3 sequence of CO and is in a region of minimal CN absorption.

The Δv=-1 bands of the red CN system also occur throughout the H region

and are observed to be quite strong in the Connes spectrum of  $\alpha$  Ori. We chose a bandpass centered at  $6512 \text{ cm}^{-1}$  to measure CN. Although CN is not particularly strong within the bandpass, the region is free of strong OH P branch lines. Our continuum point centered at  $6470 \text{ cm}^{-1}$  contains a minimum of CN as can be seen in the illustrations of Weinberg (1967) and has little OH.

The  $\Delta v=3$  sequence of CO is quite weak in stars earlier than about M0. In M stars these bands are good for abundance measurements since they are far less saturated than the fundamental or first overtone lines. Our bandpass at  $6253.7 \text{ cm}^{-1}$  measures the CO (5,2) bandhead. OH, CN, and atomic lines all occur only weakly within the bandpass. Our continuum sideband is centered at  $6273.5 \text{ cm}^{-1}$  and is somewhat depressed primarily due to atomic lines.

We have selected a bandpass centered at  $5647 \text{ cm}^{-1}$  to attempt to measure the Ballik-Ramsay (0,0) R branch heads of  $\text{C}_2$ . Although we have been unable to identify these bands at high resolution, it may be possible to measure them photometrically in G and K stars as Alexander and Branch (1974) have done using the Swan system. Our continuum point at  $5713 \text{ cm}^{-1}$  is in a relatively clean spectral region.

Stellar water absorption occurs only in stars later than about M6 as can be seen in the medium resolution spectra of Johnson and Mendez (1970) and Hyland (1974). Several combinations of spectral points in both the H and K regions should provide suitable water indices.

K BAND REGION (2.0-2.4 $\mu$ ). The most prominent features in this window are the  $\Delta v=2$  bands of CO. These bands are visible in almost all late type stars and increase rapidly in strength to later types.

Three of our bandpasses serve to measure CO in this region. One point measures the  $^{12}\text{CO}$  (2,0) head and should be useful in defining the marginal presence of CO and in measuring abundances in stars earlier than K0. In later type stars this band saturates and is less sensitive to abundance. We have included a second  $^{12}\text{CO}$  bandpass which measures primarily (4,2) band lines. It is centered at  $4232 \text{ cm}^{-1}$  and includes a larger number of weak lines. To obtain an estimate of the isotopic abundance ratio  $^{12}\text{C}/^{13}\text{C}$ , we have included a bandpass centered on the  $^{13}\text{CO}$  (2,0) head. When calibrated, this bandpass should provide a measurement of the  $^{12}\text{C}/^{13}\text{C}$  ratio in K stars.

At intermediate resolution ( $\sim 10 \text{ cm}^{-1}$ ) no useable continuum points exist within the CO band region. We have chosen to measure three continuum points shortward of the CO bands and extrapolate the continuum into the CO depressed region.

L BAND REGION (3.3-4.1 $\mu$ ). We measure only SiO in this region. Two bandpasses have been selected within the R branch of the (2,0) vibration-rotation band and one continuum point centered at  $2502 \text{ cm}^{-1}$  slightly shortward of the SiO system.

### III. INSTRUMENTATION

Observations for this program are being made on the 1.3-m Kitt Peak National Observatory telescope using a liquid-nitrogen cooled InSb grating

spectrometer. Limiting K magnitude for the program is about 4.0.

#### IV. INTERPRETATION OF THE DATA

The observational goal of this program is to define the behavior of these molecular bands in a relatively large (200-300) sample of late type stars. We plan to determine the behavior of these molecular band features with respect to temperature and luminosity and will be looking for stars in which bands are observed to be abnormally strong or weak for their spectral type. Along with "normal" oxygen-rich stars our observing program includes peculiar stars such as metal poor, CN strong, CN weak, SMR, high velocity, and S-type stars.

To aid in interpreting the observational data in terms of elemental abundances, the synthetic spectra program of Sneden (1974) will be used in conjunction with model atmospheres to synthesize the bandpasses of our program. The stars for which FTS data are available will serve as standard stars in our analysis.

TABLE I

#### INFRARED SCANNER BANDPASSES

Central Wavenumber	Bandwidth	Feature	Primary Contaminants
2493.7 $\text{cm}^{-1}$	5.5 $\text{cm}^{-1}$	SiO (2,0)	Atmospheric N <sub>2</sub> O
2496.0	5.5	SiO (2,0) head	Atmospheric N <sub>2</sub> O
2502.0	5.5	Continuum	Atmospheric N <sub>2</sub> O
4232.0	7.9	<sup>12</sup> CO (4,2)	<sup>13</sup> CO lines + Atmospheric lines
4263.0	8.0	<sup>13</sup> CO (2,0)	<sup>12</sup> CO lines + Atmospheric lines
4354.0	8.4	<sup>12</sup> CO (2,0)	Atmospheric lines
4386.0	8.5	Continuum	---
4518.5	9.0	Continuum	---
4757.0	10.0	Continuum	---
5647.0	14.0	C <sub>2</sub> BR (0,0) head	Atmospheric H <sub>2</sub> O
5713.0	14.4	Continuum	Atmospheric H <sub>2</sub> O
5956.0	10.4	Continuum	CO ( $\Delta v=3$ ) lines
6253.7	11.4	<sup>12</sup> CO (5,2) head	Atmospheric CO <sub>2</sub>
6273.5	11.5	Continuum	Atomic lines + <sup>13</sup> CO (3,0) head
6470.0	12.4	Continuum	CN ( $\Delta v=-1$ ) lines
6501.0	12.4	OH (4,2) head	CN ( $\Delta v=-1$ ) lines
6512.0	12.4	CN $\Delta v=-1$	---

#### REFERENCES

- Alexander, J.B. and Branch, D. 1974. MNRAS 167, 539.  
 Connes, P. and Michel, G. 1974. Ap. J. 190, L29.  
 Hyland, A.R. 1974. Highlights of Astronomy 3, 307.  
 Johnson, H.L. and Mendez, M.E. 1970. Astron. J. 75, 785.  
 Lambert, D.L., Dearborn, D.S., and Sneden, C. 1974. Ap. J. 193, 621.  
 Lambert, D.L. and Tomkin, J. 1974. Ap. J. 194, L89.  
 Ridgway, S. 1976. Private communication.  
 Sneden, C. 1974. PhD dissertation, U. of Texas.  
 Weinberg, J.M. 1967. PhD dissertation, Ohio State University.

## OBSERVATIONS OF FIRST-OVERTONE SILICON MONOXIDE BANDS IN COOL STARS

ROBERT F. WING AND CURTIS P. RINSLAND

Ohio State University, Columbus, Ohio

RICHARD R. JOYCE

Kitt Peak National Observatory, Tucson, Arizona

## I. INTRODUCTION

As a part of the program of infrared spectrophotometry described in the accompanying paper by Rinsland, Wing, and Joyce, we have scanned the region of the 4- $\mu$  first-overtone bands of silicon monoxide in representative late-type stars. For 18 of the brighter stars we obtained 51-point scans from 3.98  $\mu$  to 4.07  $\mu$ , a region large enough to include both the (2,0) and the (3,1) bands of  $^{28}\text{Si}^{16}\text{O}$ . Observations limited to the (2,0) band were obtained for 71 additional stars.

The observations were made in September and October, 1976, with the 1.3-m telescope at Kitt Peak National Observatory and the InSb grating spectrometer originally built for aircraft solar eclipse observations by D.N.B. Hall and recently rebuilt for stellar and nebular work by Joyce.

Observations of the first-overtone SiO bands have been reported by Cuda-back, Gaustad, and Knacke (1971), Wollman *et al.* (1973), Beer, Lambert, and Sneden (1974), and Hinkle *et al.* (1976). These studies, however, dealt with small numbers of stars, and little is known about the variation of SiO band strength with spectral type, luminosity class, or metallicity. Also, little information is available as to other absorption features which might affect photometric measurements made in this region. We therefore decided to conduct a survey of cool stars before selecting bandpasses for the program described in the accompanying paper.

The region near 4  $\mu$  is nearly free of terrestrial water absorption but is pervaded by weak lines of nitrous oxide. One objective of our survey was to measure the N<sub>2</sub>O absorption at different wavelengths and air masses and to determine how much can be tolerated for a given photometric accuracy.

II. SCANS OF THE 3.98-4.07  $\mu$  REGION

Several bright stars were scanned from 3.98 to 4.07  $\mu$ . Integrations were made at 51 points separated by approximately 1  $\text{cm}^{-1}$  or 16  $\text{\AA}$ ; the 0.5 mm exit slot gave a bandpass of 88  $\text{\AA}$  or 5.5  $\text{cm}^{-1}$ .

Giants. Figure 1 shows the spectra obtained for 5 giants of types K2 to M8 and luminosity classes III and II. The data are presented on a magnitude scale, on the instrumental system; the fall-off of all the spectra toward longer wavelengths is due largely to a local feature in the transmission function of the filter used to block spectra of higher orders. The noise level can be judged from the fluctuations of adjacent spectral points, since the bandpass is about five times the step size, while the uncertainty in the

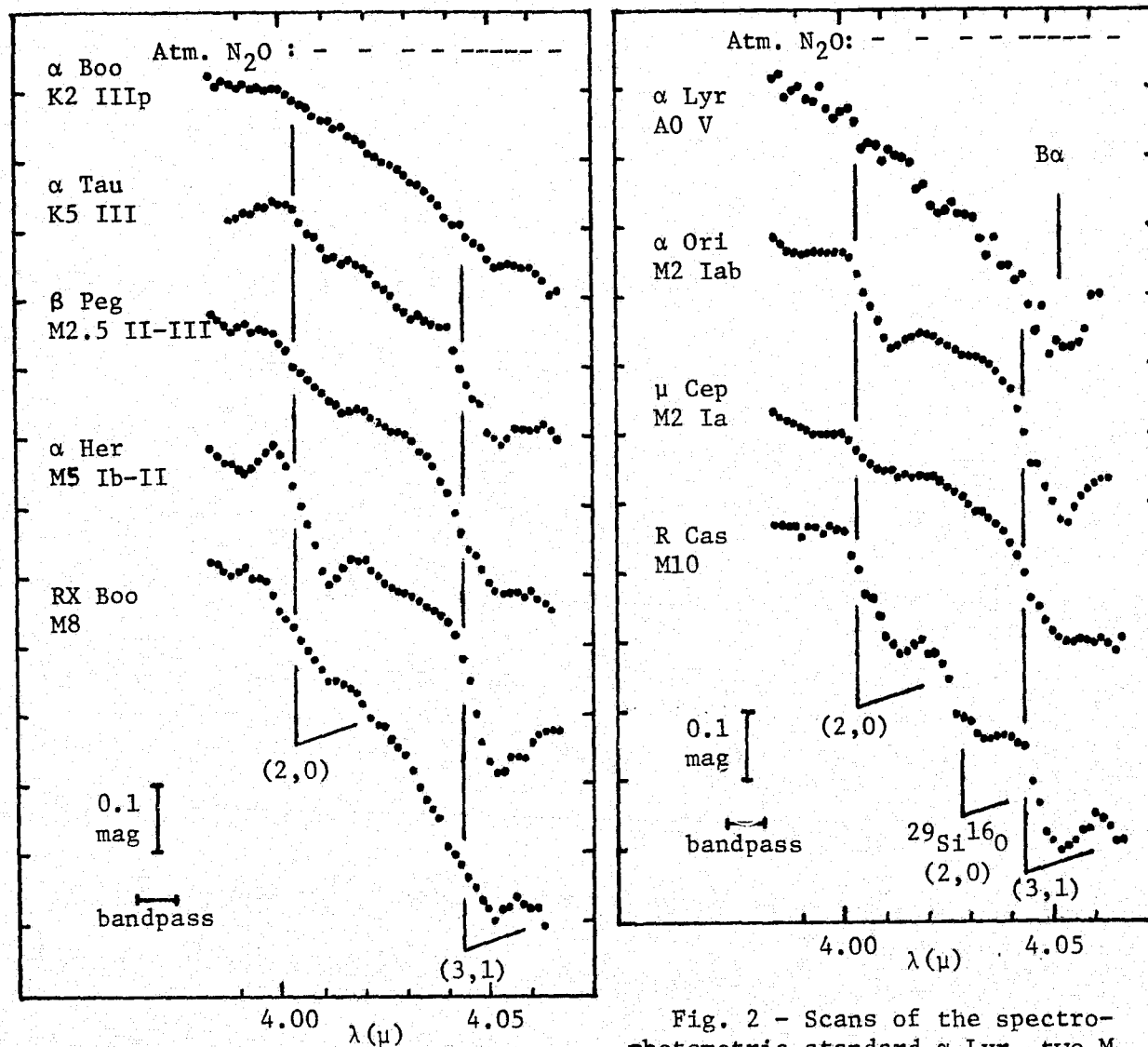


Fig. 1 - Scans of six giant stars of types K2 to M8 in the region of the SiO (2,0) and (3,1) bands. Instrumental magnitude is plotted against wavelength.

Fig. 2 - Scans of the spectrophotometric standard  $\alpha$  Lyr, two M supergiants, and the Mira variable R Cas near minimum light. The positions of Brackett  $\alpha$  and the (2,0) head of the isotopic molecule  $^{29}\text{Si}^{16}\text{O}$  are indicated.

wavelength scale of each spectrum is about equal to the step interval. The SiO bands are not definitely present in  $\alpha$  Boo, but they appear clearly in  $\alpha$  Tau and strengthen with advancing type until at least M5. A general increase in SiO strength with decreasing temperature was also found by Wollman *et al.* (1973), who measured the (3,1) band. Surprisingly, our spectra show weaker SiO features in RX Boo (M8) than in  $\alpha$  Her (M5), whereas Wollman *et al.* found RX Boo to have a stronger (3,1) band than any star of earlier type. Other giant stars which we have scanned in this manner are  $\alpha$  Cas (K0 III),  $\alpha$  UMa (K0 III), and  $\delta$  Oph (M0.5 III).

M Supergiants. Similar scans were obtained for the supergiants  $\alpha$  Ori (M2 Iab), 119 Tau (M2 Ib), RW Cyg (M3 Ia), and  $\mu$  Cep (M2 Ia). The first

three of these show stronger SiO bands than giants of similar temperatures, but the very luminous star  $\mu$  Cep has remarkably weak bands. This is shown in Figure 2, where  $\mu$  Cep is compared to  $\alpha$  Ori. Very likely the bands in  $\mu$  Cep are filled in by emission from the circumstellar envelope. This explanation was also proposed by Wollman *et al.* (1973) to account for their inability to detect SiO in the luminous stars NML Cyg and VX Sgr.

**Mira Variables.** Four Mira variables were scanned: R Cas (pure M),  $\chi$  Cyg (mild S), R Cyg (nearly pure S), and W Aql (pure S). At the time of observation, R Cas was close to minimum light ( $V \sim 13.0$ ), at which phase its spectral type is M10 by definition (Wing and Lockwood 1973). Its spectrum (Figure 2) shows very strong SiO (2,0) and (3,1) bands and, in addition, a band approximately midway between them. The latter feature also appears in several spectra of Miras obtained by Hinkle *et al.* (1976) and was identified by them as the (2,0) band of the isotopic molecule  $^{29}\text{Si}^{16}\text{O}$ . The S stars R Cyg and W Aql, both at advanced phases, also show strong SiO features, probably including the isotopic band, but their spectra are rather noisy. Our spectrum of  $\chi$  Cyg, taken at an intermediate phase, also displays strong SiO features but with little evidence of the isotopic band. The observations of Hinkle *et al.* show that the SiO bands in Miras are strongly variable.

### III. ADDITIONAL MEASUREMENTS OF THE (2,0) BAND

For 71 additional stars, measurements of the (2,0) SiO band were made with integrations at a smaller number of wavelengths. Most of these stars were observed on an 8-point program, and a few were observed at just the 3 points finally selected for the program described in our other paper. Many of these stars were observed repeatedly to help in the establishment of a photometric system. A first look at these data allows the following conclusions to be drawn:

- (1) In K stars of all luminosities the SiO bands are weak and difficult to measure at this resolution.
- (2) All M giants have detectable SiO bands; they are invariably quite strong in stars of types M4-M6.
- (3) M supergiants usually show stronger SiO bands than giants of the same temperature;  $\mu$  Cep, mentioned earlier, is an exception.

We hope that further trends, including the dependence of SiO band strength upon metallicity, will become clear once the formal reductions of the material have been carried out.

### REFERENCES

- Beer, R., Lambert, D. L., and Sneden, C. 1974, *P.A.S.P.*, **86**, 806.  
 Cudaback, D. D., Gaustad, J. E., and Knacke, R. F. 1971, *Ap.J.*, **166**, L49.  
 Hinkle, K. H., Barnes, T. G., Lambert, D. L., and Beer, R. 1976, *Ap.J.* (in press).  
 Wing, R. F., and Lockwood, G. W. 1973, *Ap.J.*, **184**, 873.  
 Wollman, E. R., Geballe, T. R., Greenberg, L. T., Holtz, J. Z., and Rank, D. M. 1973, *Ap.J.*, **184**, L85.

Airborne Infrared Spectra (2900-5600 $\text{cm}^{-1}$ ) of Stars and Planets - Lewis L. Smith and Theodore Hilgeman, Research Department, Grumman Aerospace Corporation, Bethpage, New York 11714

Infrared spectra have been obtained on several stars and planets using a Michelson interferometer mated to a Grumman designed f/23 30 cm folded Dall-Kirkham telescope aboard a NASA Lear Jet flying at an altitude of 13.7 km. The spectra of  $\alpha$  Ori, Mira,  $\alpha$  Tau, and Mars in the region 2900-5600  $\text{cm}^{-1}$  are discussed.

The absolute flux is obtained by dividing the observed stellar spectrum by a lunar spectrum, multiplying by a calculated relative lunar flux curve assuming a 350 $^{\circ}$ K blackbody and an albedo of 0.08 (Russell et al, ApJ 198, 141, 1975) and fitting the flux at 4545  $\text{cm}^{-1}$  (2.2  $\mu\text{m}$ ) to the measured K magnitude. This technique does not correct completely for the telluric bands that are saturated such as  $\text{CO}_2$  at 3550-3750  $\text{cm}^{-1}$ , hence this region has therefore been left out of the figures. A correct analysis for telluric  $\text{CO}_2$  and  $\text{H}_2\text{O}$  has to be done by a line by line atmospheric modeling program and this is now being developed.

Figure 1 is a spectra of  $\alpha$  Ori (K = -4.00) on 5 Feb 1976 at 13.3  $\text{cm}^{-1}$  resolution (solid lines). The ordinate is the absolute flux in Janskys ( $10^{-26}$  watts/meters $^2/\text{H}_2$ ) and the abscissa is in wavenumbers ( $\text{cm}^{-1}$ ). A theoretical model atmosphere with  $T_e = 3500^{\circ}\text{K}$ ,  $\log g=0$  by Fay and Johnson, (ApJ 181, 851, 1973) (dashed curve) has been fit to the observed data and shows good agreement with the depression caused by the hot CO bands in the region 4300-4400  $\text{cm}^{-1}$ . Our observations disagree with the model in the region 2900-3500  $\text{cm}^{-1}$  and this discrepancy may be important to further theoretical work. Figure 2 is a spectrum of Mira (K = -3.0) for 12 Feb 1976 at 13.3  $\text{cm}^{-1}$  resolution (solid line). A theoretical model by Auman (ApJ 157, 799, 1969) (dashed curve) with  $T_e = 2000^{\circ}\text{K}$ ,  $\log g = -2$  has been fit to the observed data and shows good agreement with the hot steam bands centered at 3700 and 5300  $\text{cm}^{-1}$ , but has too much flux in the region 3900-4500  $\text{cm}^{-1}$ . This is to be expected as no CO band absorption was included in the model. Figure 3 is a spectrum of  $\alpha$  Tau (K = -2.81) at 7.3  $\text{cm}^{-1}$  resolution on 6 Feb 1976 with the first overtone bands of  $12_{\text{C}} 16_0$  and  $13_{\text{C}} 16_0$  shown. The line identifications are facilitated using sinc apodization, though the line shapes are distorted. Mars (K = -2.0) is shown in Fig. 4 for 11 Feb 1976 at 13.3  $\text{cm}^{-1}$  resolution. The  $\text{CO}_2$  bands at 4800-5100  $\text{cm}^{-1}$ ,  $\text{H}_2\text{O}$  bands at 3800-4000  $\text{cm}^{-1}$ , and water of hydration bands at 2900-3750  $\text{cm}^{-1}$  are shown. A line by line modeling program will provide an analysis of these bands. This modeling is necessary as the vibration-rotation lines of  $\text{CO}_2$  are saturated in both the telluric and Martian spectra, and therefore add in a non-linear way.

This work has been partially supported under NASA contract NAS 2-8664.

## ALPHA ORI 5 FEB 1976

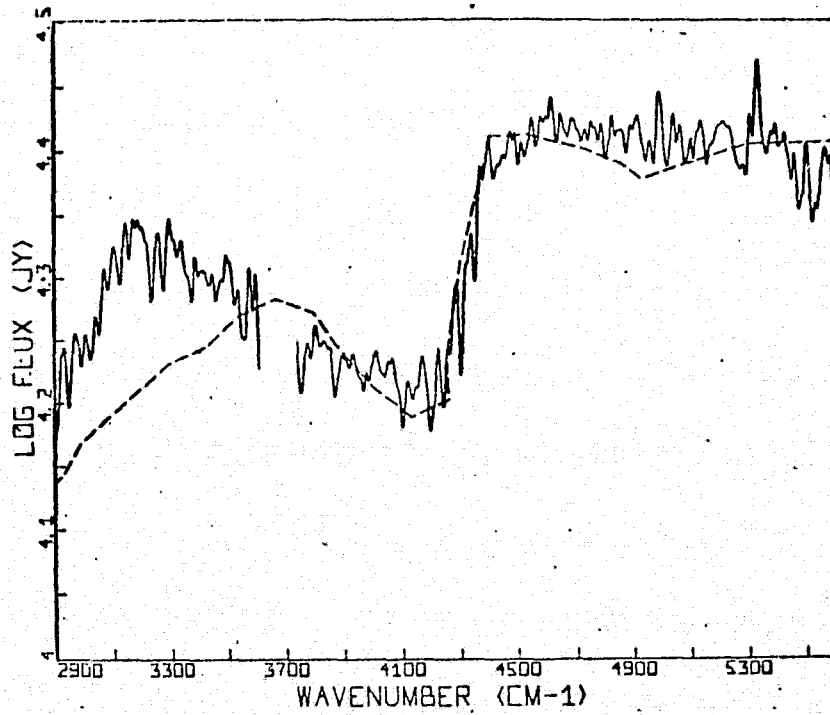


Figure 1 Spectrum Of  $\alpha$  Ori, 5 Feb 1976 With Spectral Resolution  $13.3 \text{ cm}^{-1}$  (Solid Line). Flux Is In Janskys ( $10^{-26} \text{ Watts/Meters}^2/\text{Hz}$ ). A Theoretical Model of Fay and Johnson 1973 (dashed curve) Has Been Fit To Observed Data And Shows Good Agreement With CO Depression at  $4300\text{-}4400 \text{ cm}^{-1}$  But Does Not Fit Well In The  $2900\text{-}3500 \text{ cm}^{-1}$  Region

## MIRA 12 FEB 1976

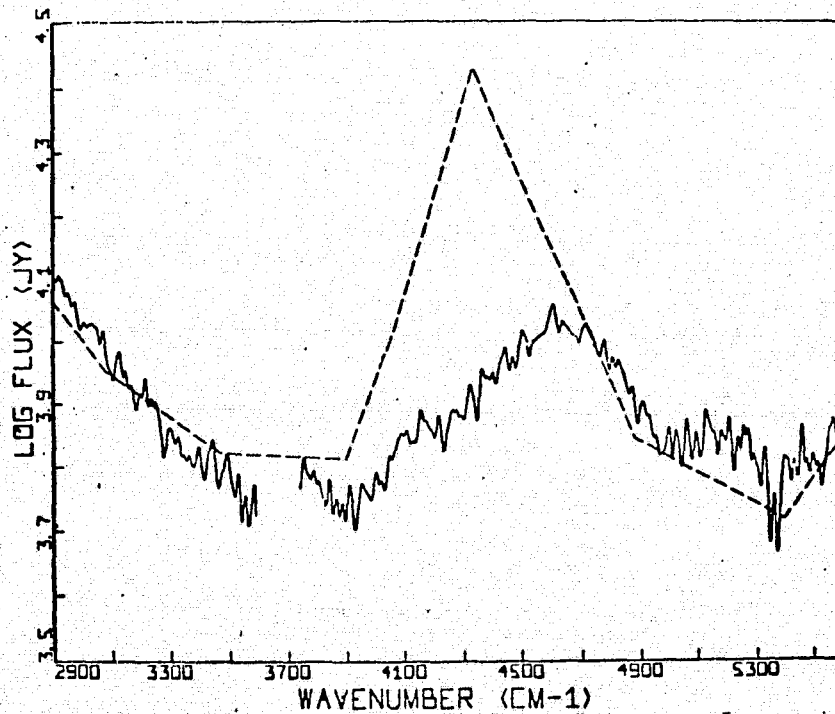


Figure 2 Mira ( $\alpha$  Ceti), 12 Feb. 1976 With Spectral Resolution  $13.3 \text{ cm}^{-1}$ . (Solid Line). A Theoretical Model Of Auman, 1969 (Dashed Curve) Has Been Fit To Observed Data And Shows Good Agreement With Hot Water Bands Centered at  $3700$  and  $5300 \text{ cm}^{-1}$ , But The Model Predicts Too Much Flux In Region Of  $3900\text{-}4500 \text{ cm}^{-1}$ . This Is To Be Expected as No CO Band Absorption Was Included In Model

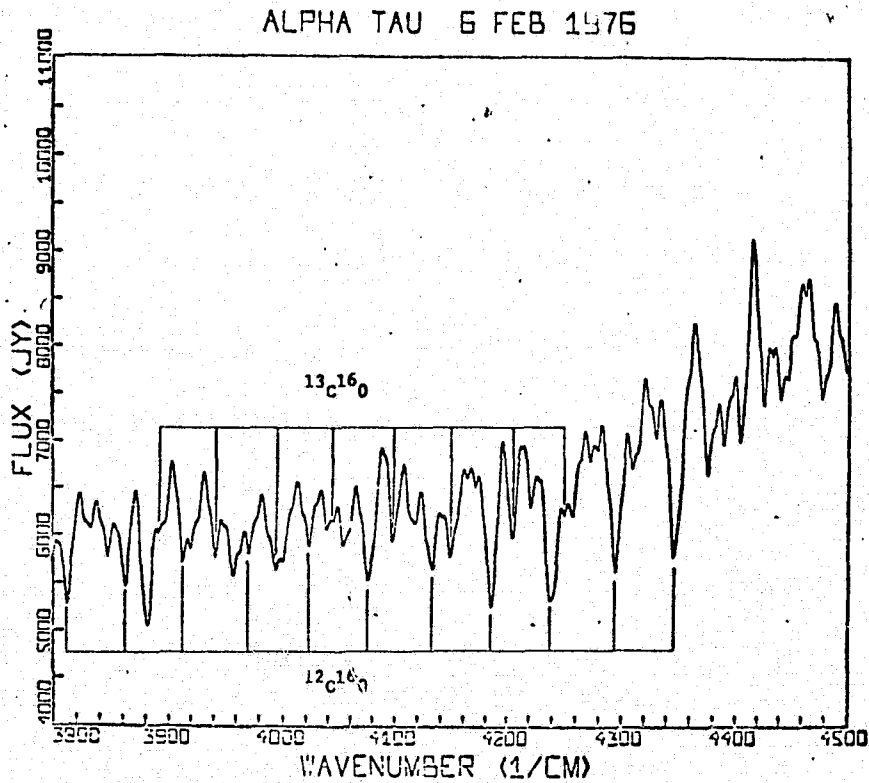


Figure 3 CO Bands of  $\alpha$  Tau, From Fig. 7 With Spectral Resolution  $7.3 \text{ cm}^{-1}$ . (Sinc Apodization). The First Overtone Bands of  $^{12}\text{C}^{16}\text{O}$  And  $^{13}\text{C}^{16}\text{O}$  Are Shown

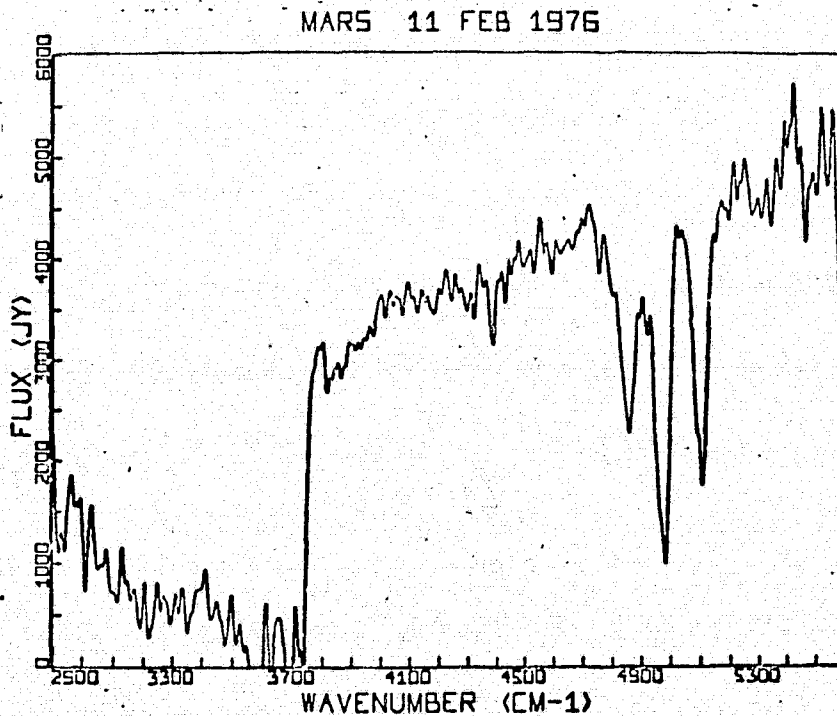


Figure 4 Spectrum Of Mars, 11 Feb. 1976 With Spectral Resolution  $13.3 \text{ cm}^{-1}$ .  $\text{CO}_2$  Bands At  $4800\text{-}5100 \text{ cm}^{-1}$ ,  $\text{H}_2\text{O}$  Bands At  $3800\text{-}4000 \text{ cm}^{-1}$ , And Water Of Hydration Bands  $2900\text{-}3750 \text{ cm}^{-1}$  Are Shown

## Spectrophotometry of OH 26.5+0.6

W. J. Forrest\*, F. C. Gillett<sup>†</sup>, J. R. Houck\*, J. McCarthy\*,  
K. M. Merrill<sup>‡</sup>, J. L. Pipher\*\*, R. C. Puetter<sup>††</sup>, R. W. Russell<sup>††</sup>,  
 B. T. Soifer<sup>††</sup>, and S. P. Willner<sup>††</sup>

## ABSTRACT

Observations of OH 26.5+0.6 (= CRL 2205 = UOA 19), a type II OH source, from 2.1 to 40  $\mu$  are reported. The observations from 4 to 8  $\mu$  and from 16 to 40  $\mu$  were made at the Kuiper Airborne Observatory; the 2 to 4  $\mu$  and 8 to 13  $\mu$  observations used ground-based telescopes at Mt. Lemmon and Kitt Peak. The spectral resolution was  $\Delta\lambda/\lambda = 0.015$  for  $\lambda < 25 \mu$  and  $\Delta\lambda/\lambda = 0.08$  for  $\lambda > 25 \mu$ ; 7" to 30" apertures were used. Airborne observations were made in the spring of 1976; ground-based observations were obtained between 1974 May and 1976 June.

The results are presented in Fig. 1, which shows the spectrum obtained in the spring of 1976. The spectrum approximates a 375 K black-body at all wavelengths. The largest deviations from a smooth continuum are the strong silicate absorptions centered at wavelengths of 10 and 18  $\mu$ . The 18  $\mu$  absorption appears weaker relative to that at 10  $\mu$  than would be expected from spectra of lunar or meteoritic silicates. Two much weaker features at 2.5 and 3.1  $\mu$  are tentatively identified as absorption by CO and H<sub>2</sub>O, respectively, in a stellar photosphere. If these identifications are correct, a minimum of 70 magnitudes of visual extinction would be required to explain the observed redness of the 2 to 4  $\mu$  continuum. In order to make these features more prominent, Fig. 1 also shows the 2 to 4  $\mu$  spectrum de-reddened by an amount corresponding to a visual extinction of 105 magnitudes.

In addition to the data in Fig. 1, the earlier ground-based observations showed that the source is variable on a time scale of months. Furthermore, when the flux is at its lowest level, the 10  $\mu$  absorption is relatively deeper and the 2 to 4  $\mu$  continuum is redder.

---

\*Cornell University

<sup>†</sup> Kitt Peak National Observatory, operated by AURA, Inc., under contract with the National Science Foundation

<sup>‡</sup> University of Minnesota

\*\*University of Rochester and Visiting Astronomer, Kitt Peak National Observatory

<sup>††</sup> University of California, San Diego

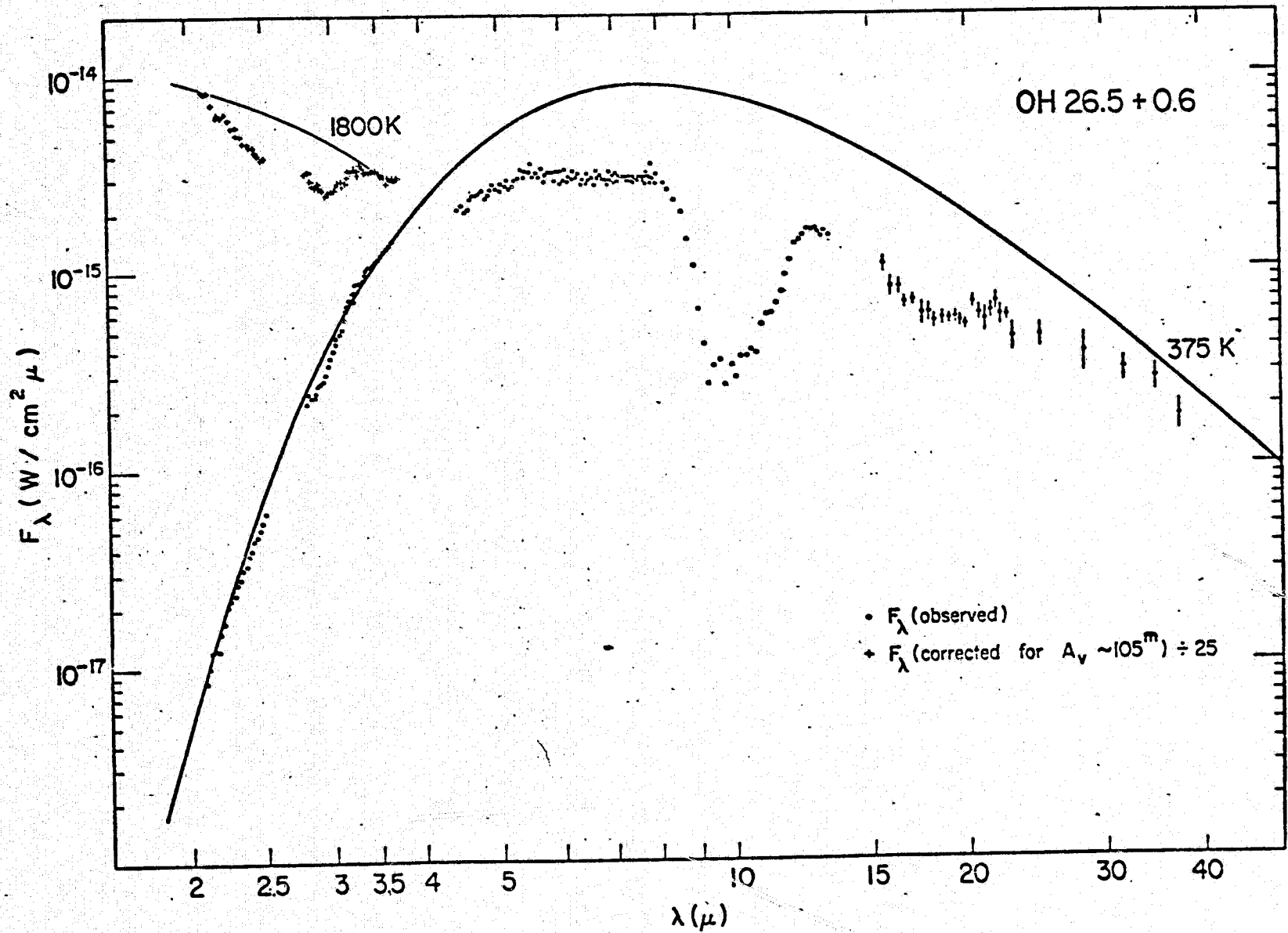


Fig. 1. The 2-40  $\mu$  spectrum of OH 26.5+0.6 obtained in May/June 1976.

The observations of OH 26.5+0.6 suggest a model of the source as a central variable star surrounded by a cloud of gas and dust that is reradiating the stellar luminosity at infrared wavelengths. The type II OH classification, the variability, and the lack of nearby young objects suggest that we are observing a star in the late stages of stellar evolution undergoing large mass loss. As the stellar luminosity decreases, the temperature of the surrounding dust decreases. The emission from the dust then decreases the most at the shortest wavelengths and in the center of the  $10 \mu$  absorption.

Various parameters can be derived from the observations and the model. If the kinematic distance of 2 kpc is correct, the luminosity is about  $3 \times 10^4 L_{\odot}$  and the mass loss rate is  $1.5$  to  $4 \times 10^{-5} M_{\odot} \text{ yr}^{-1}$ . If a typical size,  $3 \times 10^{16}$  cm, for the OH source represents the size of the shell, the time scale is  $10^3$  yr and  $\sim 2 \times 10^{-2} M_{\odot}$  of gas and silicate dust have been ejected into the interstellar medium.

Presumably the dust in OH 26.5+0.6 is typical of oxygen-rich material in the interstellar medium. The observations show that such material has a significant opacity at wavelengths shorter than  $8 \mu$ .

#### ACKNOWLEDGEMENTS

Airborne Infrared Astronomy is supported by NASA grants NGR 33-010-081 at Cornell University and NGR 05-005-055 at UCSD. J.P. acknowledges financial support from an NSF grant. The UCSD-U. Minn. Mt. Lemmon Observatory is supported by grants from the NSF and NASA.

## Abstract

## The Spectrum of IRC 10216 from 2.0 to 8.5 Microns

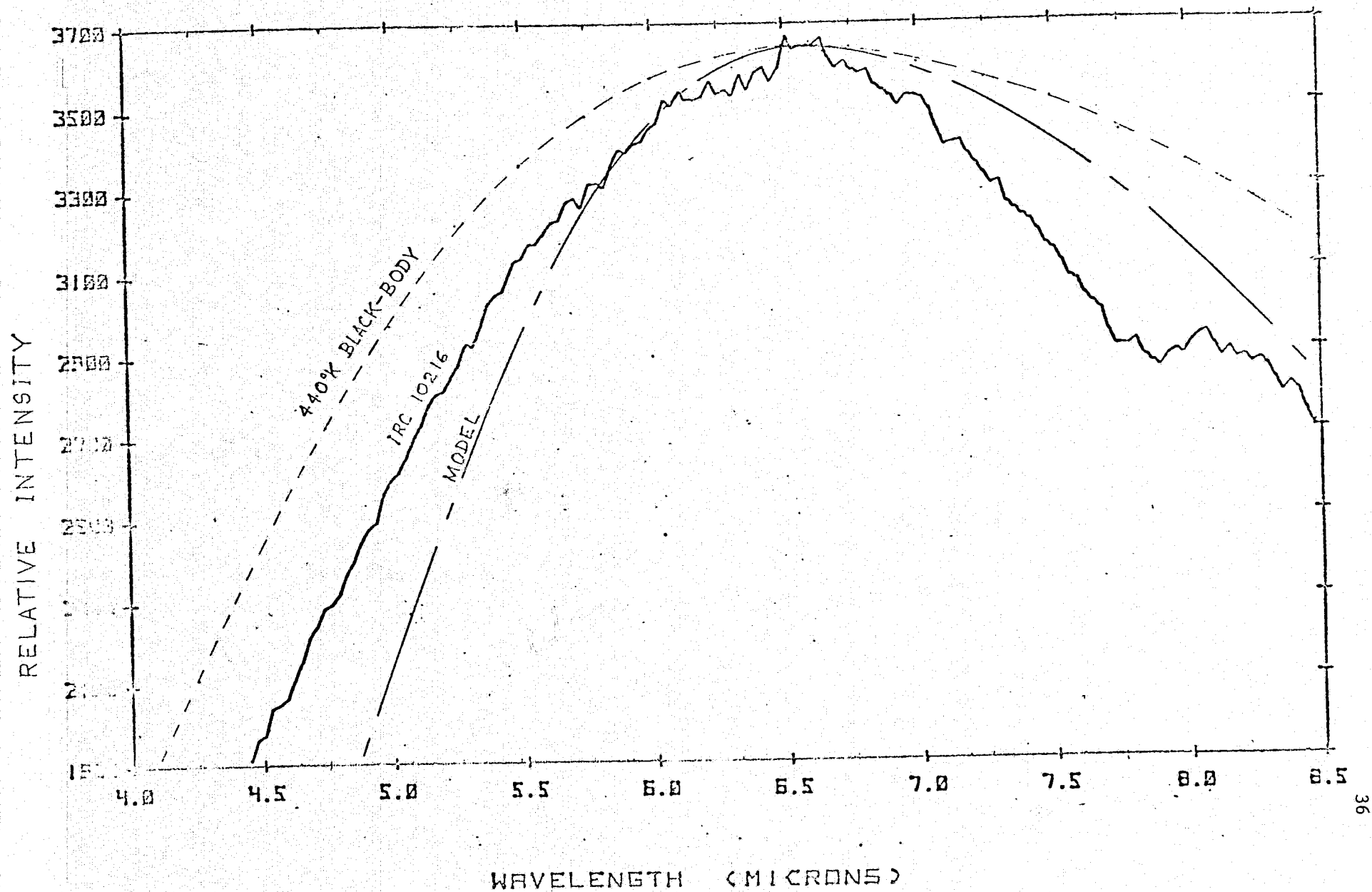
by

F.C. Witteborn, D.W. Strecker, E.F. Erickson, S.M. Smith, and J.H. Goebel  
 NASA-Ames Research Center, Moffett Field, CA 94035

Spectra of IRC 10216 covering the ranges 2.0 to 4.1 and 4.4 to 8.5 microns were obtained using cooled filter wedge spectrometers with the Kuiper Airborne Observatory (KAO) at 41,000 feet. The transmission of the short wavelength system, used on January 5, was calibrated by obtaining spectra of  $\alpha$ Tau on the same flight. The long wavelength spectra, obtained on January 23, can be compared with spectra of Mars taken during the same flight. However, because of uncertainties in the emissivity of Mars in the 4-8 micron range, the instrument function and a typical atmospheric transmission function were determined on a later flight by taking spectra of the sun with the same instrument from the same altitude. In this case the solar intensity was reduced by stopping the KAO telescope down to 3" diameter and by using a spectrally calibrated neutral density filter with a transmission of about  $10^{-3}$ . The spectral resolution of the spectrometers is about 2%. Absolute flux calibrations and a more refined correction for atmospheric absorptions are planned but not yet completed.

The spectrum is featureless except for an absorption near 3.1 microns reported previously by K.M. Merrill and W.A. Stein (P.A.S.P. 88, 294, 1976) and an absorption near 7.8 microns which may be of terrestrial origin. The 4.5 to 8.5 micron portion of the spectrum shown in figure 1 is narrower than a blackbody and peaks at 6.6 microns. A 440°K blackbody is shown for comparison. Also shown is a spectrum of a model dust envelope calculated by T.W. Jones and K.M. Merrill (Astrophys. Jour. 209, 509, 1976). The model chosen for comparison is for a graphite outer shell radius 80 times that of the underlying star (whose temperature must be somewhat lower than the 2400 K used as an example by Jones and Merrill). Its optical depth  $\tau$  is 0.5 at 10 microns and varies inversely as the radius within the shell. In this model the short wavelength radiation from the warm interior is obscured by the cooler dust outside, since the opacity increases with shorter wavelengths. The long wavelength dependence of the emissivity ( $\lambda^{-1}$ ) or steeper tends to further narrow the spectrum below that of a blackbody. M.F. Campbell, et al. (Astrophys. Jour. 208, 396, 1976) have reported measurements consistent with an emissivity varying as  $\lambda^{-1}$  at long wavelengths. The relatively narrow peak of the continuum reported here is not consistent with the direct addition of the 375 K and 600 K blackbody clouds used to model the lunar occultation measurements described by R.I. Toombs, et al. (Astrophys. Jour. 173, 171, 1972), however, dual or multiple cloud models may still be necessary to explain data outside the 4.5 to 8.5 micron range.

FIGURE 1 : IRC+10216 SPECTRUM



## III. NEBULAE

### Hydrodynamic Calculation of Collapsing Interstellar Clouds

by H. Gerola, IBM Thomas J. Watson Research Laboratory and A.E. Glassgold, N.Y. Univ.

We have developed a spherical hydrodynamic program for studying the evolution of interstellar clouds which include the thermal and chemical phenomena associated with interstellar molecules. One objective is to understand the relationship between the various chemical, thermal, and dynamical time scales in collapsing clouds. Another objective is to obtain the emissivities of such clouds at different wavelengths, and to determine how they might be observed.

In addition to integrating the mass and momentum conservation equations, we solve the heat equation for a suitable composite heating and cooling model, as well as, the rate equations defining the currently accepted gas-phase in molecule chemistry. Interstellar dust grains provide the sites for forming  $H_2$  molecules, cooling warmer gas by collisions, heating the gas through photoelectrons, and attenuating interstellar UV radiation.

For gravitationally unstable clouds, a core-envelope density distribution evolves in the characteristic free fall time  $[t_f + (3\pi/32G\rho_0)^{1/2}]$ , where  $\rho_0$  is the initial density, similar to the results obtained by earlier workers. The evolution of the temperature profile is sensitive to the heating model, and the details of the calculated velocity distribution have interesting implications for the line radiative transfer problem in interstellar clouds. The chemical development is strongly influenced by the dynamical evolution. For example, the relatively long initial time scale for the development of molecular hydrogen is considerably shortened; substantial conversion from atomic to molecular hydrogen can occur in  $\sim 10^6$  y for a cloud of mass  $M=2 \times 10^4 M_\odot$ . The formation of substantial CO abundances may take longer, e.g.  $2-5 \times 10^6$  y depending on the chemistry. Considerable CI is

formed in the interior of the cloud, and the exterior regions are dominated by CII.

The occurrence of large amounts of carbon in non-molecular form raises interesting possibilities for observing collapsing clouds in the infrared. The details of the calculated density and velocity distributions will also affect the emissivity of collapsing clouds at radio frequencies.

# The Calculated Infrared Appearance of Collapsing Protostellar Clouds

H.W. Yorke

Max-Planck-Institut für Physik und Astrophysik,  
Föhringer Ring 6, 8000 München 40, FRG.

## Introduction:

The presence of powerful infrared sources imbedded in dense molecular cloud complexes have often been interpreted as massive protostars or early-type main sequence stars surrounded by thick circumstellar shells of dusty material. Here, the optical and ultraviolet radiation from the central source is absorbed by the dust and reradiated at longer wavelengths. Recently, Yorke and Krügel (1975) and (1976) have presented the results of time dependent hydrodynamic calculations for the dusty envelopes of massive protostars ( $50 M_{\odot}$  and  $150 M_{\odot}$ ), starting from the time of initial gravitational collapse and continuing until the matter in the envelope has become tenuous enough for a compact HII region to form. In the early phases of evolution after a starlike nucleus has formed at the center of the protostellar cloud, the infalling material acted as a false photosphere, absorbing all radiation at the near infrared and optical wavelengths. At first the evolution of the envelope was qualitatively similar to a series of Kahn's (1974) steady-state solutions for cocoon stars. The inner edge of the cocoon was located about  $10^{14}$  cm, which was the radius at which graphite particles melt. Later, a dense shell ( $n_{\text{H}_2} \sim 10^7 \text{ cm}^{-3}$ ) developed at approximately  $10^{17}$  cm due to the radiation acceleration on the dust particles. Inside this outer cocoon, the infalling gas became increasingly dust depleted with the passage of time.

In the following, the detailed radiation transfer problem, including scattering is solved numerically for spherically symmetric protostellar clouds during various stages of collapse. For these calculations the density distributions of gas and dust as calculated by Yorke and Krügel (1976) using a two-fluid hydrodynamic code to describe the birth of a massive star in a dense dusty cloud are used. At each point in the envelope the grain temperature, spectra, and angular distribution of the radiation are solved simultaneously assuming radiative equilibrium. The spectral as well as the spatial distribution of the radiation flux over the entire disk is presented for a  $50 M_{\odot}$  and a  $150 M_{\odot}$  protostellar cloud at various evolutionary stages up to (but not including) the development of a compact HII region. In both cases the envelope surrounding the accreting protostar (which in later stages is a main sequence star) is always opaque to the stellar photons, and the resulting appearance is that of an extended infrared source. Furthermore, it is shown that a double peaked infrared spectrum becomes more and more pronounced during the later stages of evolution after the formation of an outer dust cocoon at  $r \sim 10^{17}$  cm.

Details of the numerical method, as well as the extinction cross sections and albedo for the type of dust grains used are given in Yorke (1976).

## The IR Appearance of the 50 $M_{\odot}$ cloud.

We consider the evolutionary sequence of a collapsing 50  $M_{\odot}$  protostellar cloud with an outer radius  $r_{\max} = 8 \times 10^{17}$  cm. After  $1.02 \times 10^{13}$  s the central core has accreted 7  $M_{\odot}$  and has a luminosity of  $L = 10^4 L_{\odot}$ , over 80 % of which arises at the accretion shock front. As can be seen from the spectral distribution of the luminosity  $L_{\nu} = 4\pi r^2 F_{\nu} = (4\pi)^2 r^2 H_{\nu}$  displayed in Fig. 1, the protostellar cloud at this stage appears as an extended spot of temperature  $T \sim 50$  K with a slight excess at wavelength around  $20\mu$ . This excess comes from the central part of the disk which has the character of a heavily obscured source at a somewhat higher temperature. In Fig. 1 we display also the spectral distribution of the luminosity  $L_{\nu}$  at a later stage of evolution. At  $t = 1.12 \times 10^{13}$  s the core has a mass of 16  $M_{\odot}$  and a total luminosity  $L = 3 \times 10^4 L_{\odot}$ , 16 % of which arises from the accretion shock. The hydrodynamic calculations show also that a shell of material has formed at  $r \approx 10^{17}$  cm due to the outward motion of the dusty gas. Here, the double-peaked nature of the radiation flux has become quite apparent.

At  $t = 1.17 \times 10^{13}$  s the core is a 17  $M_{\odot}$  main sequence star of luminosity  $L = 2.5 \times 10^4 L_{\odot}$ . The outer dust cocoon has become more pronounced. In Fig. 2 the spectral distribution of the luminosity integrated over the entire disk is displayed. For comparison, the normalized fluxes from the center of the disk ( $p=0$ ) and from a region off center ( $p = 1.8 \times 10^{17}$  cm) are also given. At this point the hydrodynamic calculations were stopped. One expects a compact HII region to form inside the outer cocoon within several  $10^3$  years when the density has decreased sufficiently. It should be noted that only one third of the 50  $M_{\odot}$  of the original protostellar cloud contributed to the final mass of the resultant main sequence star. For the 150  $M_{\odot}$  protostellar cloud, this ratio was even lower (24 %).

Further results and their implications will be presented during the Symposium talk.

### References

- Kahn, F.D. 1974, *Astron. Astrophys.* **37**, 149.  
 Yorke, H.W. and Krügel, E. 1975, *Mitt.d.Astron.Ges.* **38**, 222.  
 Yorke, H.W. and Krügel, E. 1976, submitted to *Astron.Astrophys.*  
 Yorke, H.W. 1976, submitted to *Astron.Astrophys.*

### Figure Captions

Fig. 1: The spectrum of a 50  $M_{\odot}$  collapsing protostellar cloud at two different evolutionary times,  $t = 1.02 \times 10^{13}$  s and  $t = 1.12 \times 10^{13}$  s.

Fig. 2: The spectrum of a 50  $M_{\odot}$  protostellar cloud immediately preceding the development of a compact HII region ( $t = 1.17 \times 10^{13}$  s).

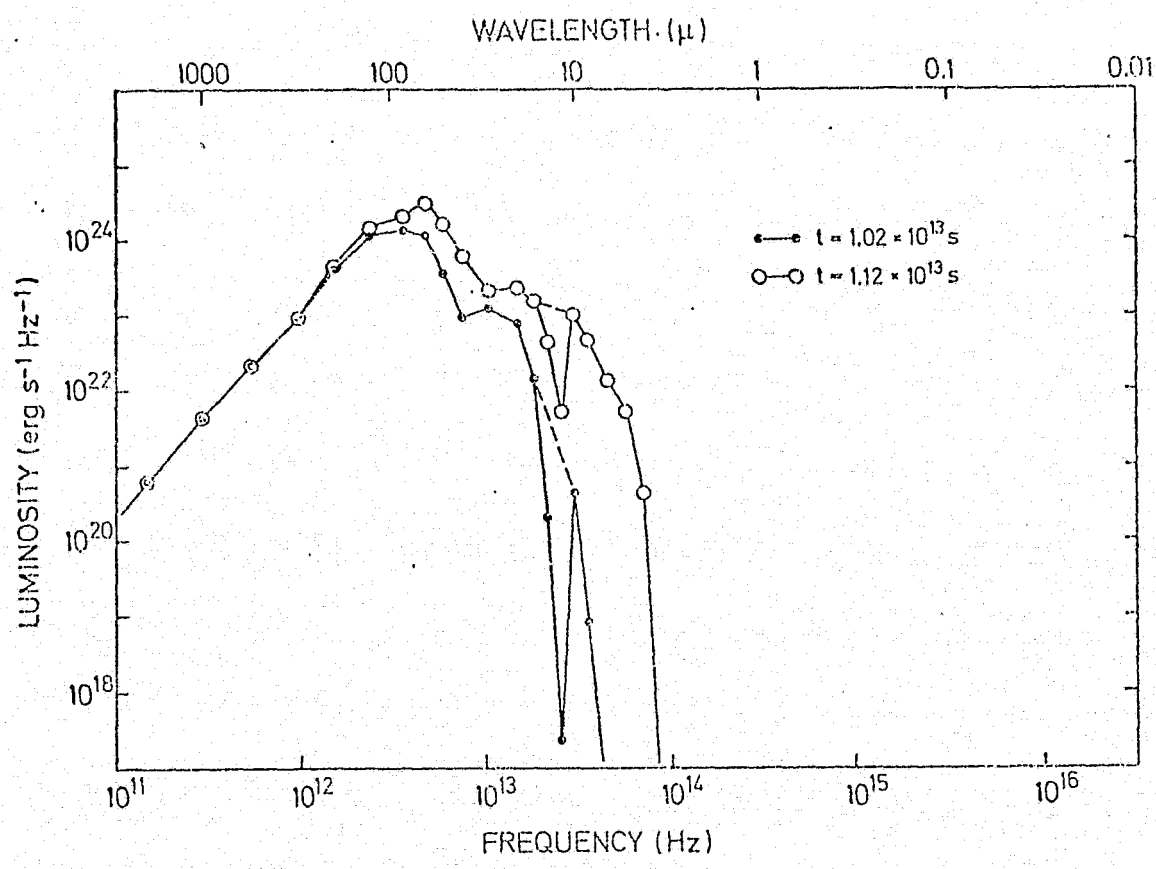


Fig. 1

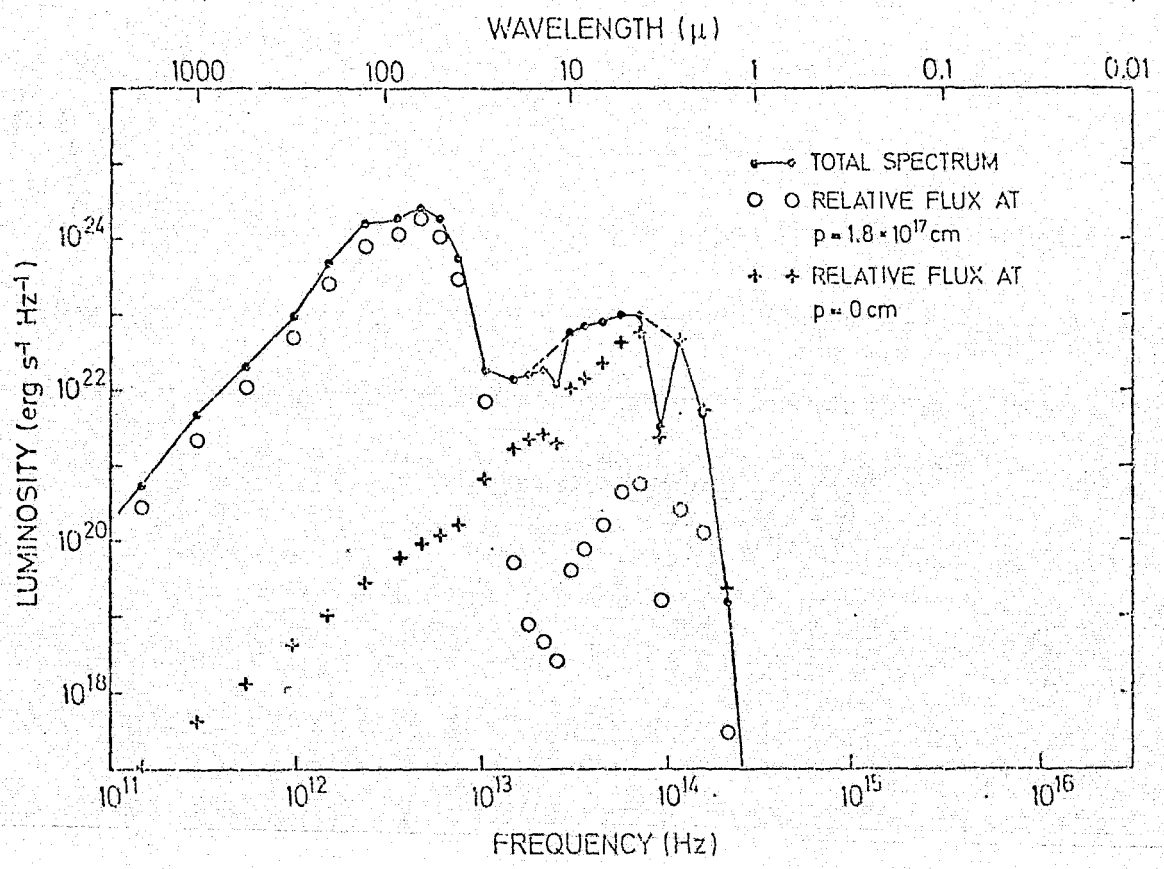


Fig. 2

DENSITY AND TEMPERATURE GRADIENTS IN SGR B2, Lawrence J. Caroff, NASA Ames Research Center, Moffett Field, CA. Westbrook, et. al (1976) have recently presented a moderately high spatial resolution map of the molecular cloud Sgr B2 in the thermal continuum at 1 mm. Under the assumption that Sgr B2 is spherically symmetric, this map and the map of Scoville, Solomon, and Penzias (1975) in the 1-0 line of  $^{13}\text{CO}$  can be combined to give the three-dimensional density and temperature profiles of the dust in the inner part of the cloud assuming that LTE obtains. At the present time the data do not merit a detailed empirical fit, so the density and temperature are taken to be proportional to  $r^{-\alpha}$  and  $r^{-\beta}$ , respectively. A straightforward, though somewhat complicated analysis gives  $\alpha$  slightly larger than one and  $\beta \approx 3/4$ . This value of  $\beta$  is somewhat larger than suggested by theory (eg Scoville and Kwan 1976). Non-LTE effects will be discussed qualitatively as will the effects of density and temperature gradients on the interpretation of the recently-obtained far-infrared spectrum of Sgr B2 (Erickson, et al, 1977).

Erickson, E.F., Caroff, L.J., Simpson, J.P., Strecker, D.W., and Goorvitch, D., 1977, "The Far Infrared Spectrum of the Core of Sgr B2," preprint.

Scoville, N.Z., Solomon, P.M., and Penzias, A.A., 1975, ApJ 201, 352.

Scoville, N.Z., and Kwan, J., 1976, Ap J 206, 718.

Westbrook, W.E., Werner, M.W., Elias, J.H., Gezari, D.Y., Hauser, M.G., Lo, K.Y., and Neugebauer, G., 1977, "One-Millimeter Continuum Emission Studies of Four Molecular Clouds," preprint.

An interpretation of the Becklin-Neugebauer  
object and related infrared point sources

P. J. Bedijn,<sup>1)</sup> H. J. Habing,<sup>2)</sup> and T. de Jong<sup>3)</sup>

- <sup>1)</sup> Sterrewacht, Leiden, The Netherlands, <sup>2)</sup> Joint Institute for Laboratory  
Astrophysics, University of Colorado and National Bureau of Standards,  
Boulder, Colorado, on leave of absence from Sterrewacht, Leiden, The  
Netherlands, <sup>3)</sup> Universiteit van Amsterdam

Some 15 infrared point sources have been discovered with spectral characteristics much like those of the Becklin-Neugebauer object in Orion (for a compilation of information see Wynn-Williams, Proceedings of the IAU Symposium on Star Formation, Genève, Switzerland, September 1976). It has frequently been suggested that these sources are protostellar objects, although detailed interpretations have not yet been given, except by Larson (M.N.R.A.S. 1969, 145, 297). Basically different interpretations have also been suggested.

We have made extensive radiative transfer calculations on a simple model and are able to predict spectra that accurately fit all existing observations of the best observed of these point sources. Our interpretation is as follows. In the final stages of the formation of massive stars there is a certain period when the star has already reached the main sequence, but cloud material is still falling in. Gradually the inflow stops and an H II region develops, signalling the end of the accretion phase. Around this time strong OH masers appear (Habing, Goss, Matthews, and Winnberg, Astron. Astrophys. 1974, 35, 1). Gas dynamical calculations for this late accretion phase have been made by Yorke and Kruegel (private communication). We suggest that the group of infrared point sources mentioned in the beginning are actually stars in this late accretion phase and that in a short time they will develop supercompact H II regions such as have been found, e.g., near NGC 7538.

The model that we use for our calculations is a much extended version of that of Larson (loc. cit.). It consists of three components: (1) a point source of luminosity  $L$  and mass  $M$ ; (2) a cloud of approximate size  $10^{16}$  cm, collapsing in free fall onto the star; (3) a surrounding molecular cloud. The surrounding cloud is too cold to emit significantly at  $\lambda < 20 \mu\text{m}$ , but it absorbs heavily at these wavelengths.

We calculate selfconsistently the temperature distribution and the emitted infrared spectrum of the grains in the collapsing cloud, and then we let this spectrum be "reddened" by the surrounding molecular cloud. The most critical parts in the calculations are

- (1) the assumed absorption characteristics of the adopted grain species,
- (2) the matching procedure of the (nonlinear) model spectra to the observations.

With respect to the grain properties we adopted two types of grains: spherical graphite particles of  $200\text{\AA}$  radius and spherical silicate grains of  $500\text{\AA}$  radius. We used the best absorption properties available in the literature. Applying our model calculations also to infrared spectra of late type giants to study the silicate absorption properties we found that we had to increase the silicate absorptivity below  $7\text{ }\mu\text{m}$ . Independently this latter conclusion has also been reached by Jones and Merrill (Ap. J. 1976, 209, 509). For the band profile around  $9.7\text{ }\mu\text{m}$  we used the shape given by Gillett and Forrest (Ap. J. 1973, 179, 483).

To mimic the grain mantles that probably exist in the surrounding cloud, we took the combined silicate and graphite extinction law and added, to a variable amount, a generalized extinction law, for which we used van de Hulst's curve no. 15.

With respect to the fitting procedure we had five free parameters available, divided over two separate parameter spaces. Several of these parameters are however restricted by circumstantial evidence, such as measurements of the total luminosity, including the far infrared, and of the parameter  $A_V/\tau_{10\mu}$ .

As an example we show in figure 1 the observation for the Becklin-Neubegauer object, together with our best spectral fit. The upper curve

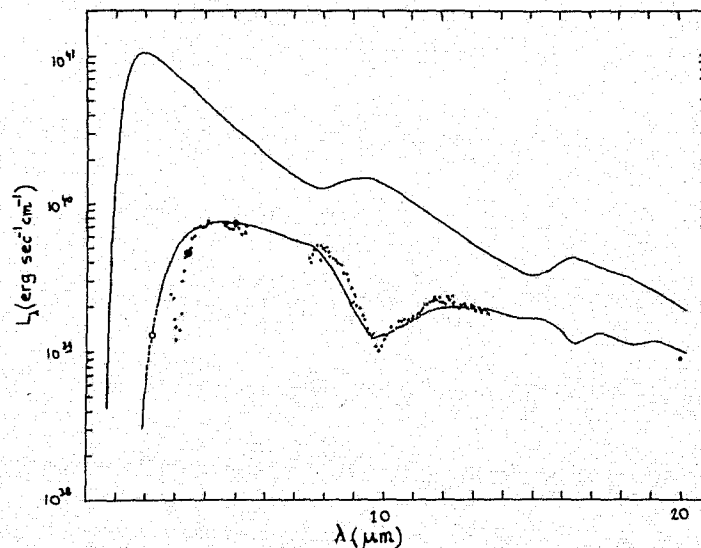


Figure 1

represents the spectrum of the collapsing cloud, the lower curve the same spectrum modified by the surrounding molecular cloud. The luminosity of the stellar object is  $L = 1.8 \times 10^4 L_\odot$  and the mass in flow rate equals  $2.2 \times 10^{-6} M_\odot$ , provided that the stellar mass is  $11 M_\odot$  and the dust-to-gas ratio (by mass) equals  $8 \times 10^{-3}$  in the collapsing cloud. The extinction by the surrounding cloud  $A_V$  equals  $59^m$  and  $A_V/\tau_{10\mu} = 23$ . Unfortunately

we did not include in our calculations the ice absorption band around  $3.5 \mu\text{m}$ , but estimates indicate that enough cool material is present in the outside cloud to explain the observed strength of this band.

A detailed account of the model calculations may be found in the Ph.D. thesis by P. J. Bedijn (1977, Leiden University).

# The Energetics of Molecular Clouds

by

N. J. Evans II and G. N. Blair  
The University of Texas at Austin  
Austin, Texas 78712

and

S. Beckwith  
California Institute of Technology  
Pasadena, California

We have begun a program to collect complete molecular line, radio continuum and infrared data on a group of relatively simple, nearby molecular clouds. We have also developed "first order" techniques to analyze the physical properties of the molecular clouds and the energetic relations between the gas and the dust content of the clouds. These include estimates of the kinetic temperature, gas density, gas cooling, and dust cooling rates. The gas and dust cooling rates are then compared to heating rates due to nearby stars and imbedded infrared sources. In this paper, these techniques will be applied to the S255 and S140 molecular clouds. Both clouds are regions of extended CO emission and both contain a single strong infrared source not associated with any HII region. The most salient results are the following. 1) The primary energy flow is in the infrared through dust emission at a range of temperatures. 2) The gas cooling rate is much less than the dust cooling rate. 3) The primary heat sources in the S255 cloud are nearby stars; in the S140 cloud, an embedded infrared source is probably more important for heating; in both clouds the infrared source is responsible for at least local heating. 4) A large far-infrared flux ( $\sim 10^3$  Jy) is predicted from both molecular clouds. 5) Both clouds show a strong enhancement of molecular density, as well as temperature, centered on the strong infrared source.

## Strong Far Infrared Emission From A Compact Source In S140

P. M. Harvey, M. F. Campbell, and W. F. Hoffmann

Steward Observatory, University of Arizona

Far infrared observations of S140 have been obtained on the NASA C-141 Kuiper Airborne Observatory. Mapping at  $90\mu$  ( $65$ - $200\mu$ ) with a  $40''$  beam and photometry at  $40$ ,  $53$ ,  $100$ , and  $175\mu$  are described. Previous radio and near infrared observations of S140 have found an extended molecular cloud with a strong  $20\mu$  infrared source embedded near one edge of the cloud adjacent to the bright rim of nebulosity which constitutes S140. We have detected one compact far infrared source which is apparently coincident with the near infrared object, the high density core of the molecular cloud, and an  $H_2O$  maser. The observed flux densities of this source at various wavelengths are:  $6780$  Jy at  $40\mu$ ,  $8190$  Jy at  $53\mu$ ,  $8590$  Jy at  $100\mu$ , and  $5440$  Jy at  $175\mu$ , all of which have negligible statistical uncertainty and  $\pm 25\%$  absolute calibration uncertainty. The object appears unresolved with a  $40''$  beam at  $100\mu$ , and unresolved or marginally resolved with a  $17''$  beam at  $53\mu$ . At an assumed distance of  $1$  kpc the infrared luminosity is  $\sim 2 \times 10^4 L_\odot$ , comparable to that of a B0 main-sequence star. A very low upper limit to the radio flux of  $5 \times 10^{-3}$  Jy from this region has previously been established, however, suggesting that this object may be quite similar to the BN object in Orion believed possibly to be a pre-stellar source. No other far infrared sources were detected in a  $7' \times 7'$  area centered on the peak down to a limit of  $300$  Jy ( $1\sigma$ ) at  $90\mu$ . This work was supported by NASA grant NGR 03-002-390.

"Far infrared observations of molecular cloud S 140 and the Galactic plane"

ROUAN D., LENA P., PUGET J.L., DE BOER K., WIJNBERGEN J.  
 Université Paris 7 et Observatoire de Meudon,  
 Space Science Group, University of Groningen.

Observations were performed during April 1976, with a 32cm open- port airborne telescope. Two filters were used of respectively 114-196 $\mu$  and 72-94 $\mu$ m bandwidth. The diaphragm was 6.3 arc min. and the beam chopping frequency was 37 Hz. Calibration was based on observation of Saturn.

1. The S 140 region

The S 140 region was observed in the area where a strong molecular emission (CO and H<sub>2</sub>O) and a near infrared point source have been previously discovered<sup>(1), (2)</sup>. We have detected, at the same location, a far infrared emission giving the following fluxes in the two bands :

$$F(114-196) = 6.4 \pm 1.5 \cdot 10^{-14} \text{ w cm}^{-2}$$

$$F(72-94) = 3.2 \pm 0.5 \cdot 10^{-14} \text{ w cm}^{-2}$$

A dust temperature of 35 K can be derived from the ratio of these two measurements assuming that dust absorption efficiency varies as  $\lambda^{-2}$  beyond 70 $\mu$ m. This temperature is in good agreement with the CO brightness temperature of 27 K if one follows proposed models of molecular clouds<sup>(3)</sup>. The total infrared flux is  $2.1 \cdot 10^{-13} \text{ w cm}^{-2}$ , a very close value to the one derived from the near infrared luminosity of the point source ( $M_v = -6.5$ ).

With reasonable hypothesis on grain composition and dust to gas ratio we find from the far infrared flux an opacity of 15 mag. This value is in good agreement with the ones deduced from CO measurements and near infrared photometry of the point source. (respectively  $A_v = 22$  and  $A_v = 30$  mag).

The S140 area offers thus a classical picture of a dense molecular cloud with embedded young stars.

The galactic plane was scanned in the 72-94 $\mu$ m band at  $\ell = 28^\circ$ , a place close to the maximum of the CO emission previously measured <sup>(4)</sup> (fig. 1). Although the guide star did not allow a complete crossing of the plane, a positive detection is reported. The measured flux is  $1.4 \cdot 10^{-4} \text{ w m}^{-2} \text{ sr}^{-1}$  (fig. 2).

The good agreement between column densities derived from CO <sup>(4)</sup>, X-ray <sup>(5)</sup> and  $\gamma$ -ray data confirms that CO is a good tracer of the total amount of matter along the line of sight, in the inner galaxy, and leads us to take  $N_H = 1.5 \cdot 10^{23} \text{ cm}^{-2}$  as the best estimate of the column density at  $b = 0$ ,  $\ell = 28^\circ$ . If the dominant contribution to the 70-95 $\mu$ m radiation comes from dust within HII regions at typical temperature of 70 K, the total infrared luminosity would be of about  $2.8 \cdot 10^{-3} \text{ w cm}^{-2} \text{ sr}^{-1}$ . This value does not agree with the  $3 \cdot 10^{-5} \text{ w cm}^{-2}$  that can be derived from the known distribution of HII regions <sup>(6)</sup>. On the other hand, if one looks for the minimum temperature which all the dust present in the line of sight must have to account for the observed flux, the value  $T_d = 22^\circ \text{ K}$  can be deduced from a semi-empirical relation <sup>(7)</sup> giving the total infrared luminosity per atom of Hydrogen :

$$L_{\text{IR}}^{\text{H}} = 6.5 \cdot 10^{-38} T_d^{5.8} \text{ w/H atom}$$

The total infrared luminosity is then  $L_{\text{IR}}^{\text{H}} = 4 \cdot 10^{-30} \text{ W/H atom}$  at

$\ell = 30^\circ$ . Thus, even with the most economical energy balance in terms of absorbed stellar radiation, we must conclude that our Galaxy has a total infrared luminosity of the order or larger than its visible luminosity.

#### REFERENCES

- (1) BLAIR, G.N., and VANDEN BOUT, P.A., 1974, Bull.AAS, 6, 452.
- (2) BLAIR, G.N., PETER, W.L., and VANDEN BOUT, P.A. 1975, Ap.J. (Letters) 200, L 161.
- (3) GOLDREICH, P., and KWAN, J. 1974, Ap.J. 189, 441.
- (4) GORDON, M., and BURTON, W., 1976, Ap.J. (in press).
- (5) RYTER, C. 1976, communication at the A.P.S. Meeting, May 1975, Washington D.C.
- (6) MEZGER, P. 1974, in "Interstellar Medium", Editor: K.PINKAU.
- (7) RYTER, C., and PUGET, J.L. 1976, submitted to Ap.J.

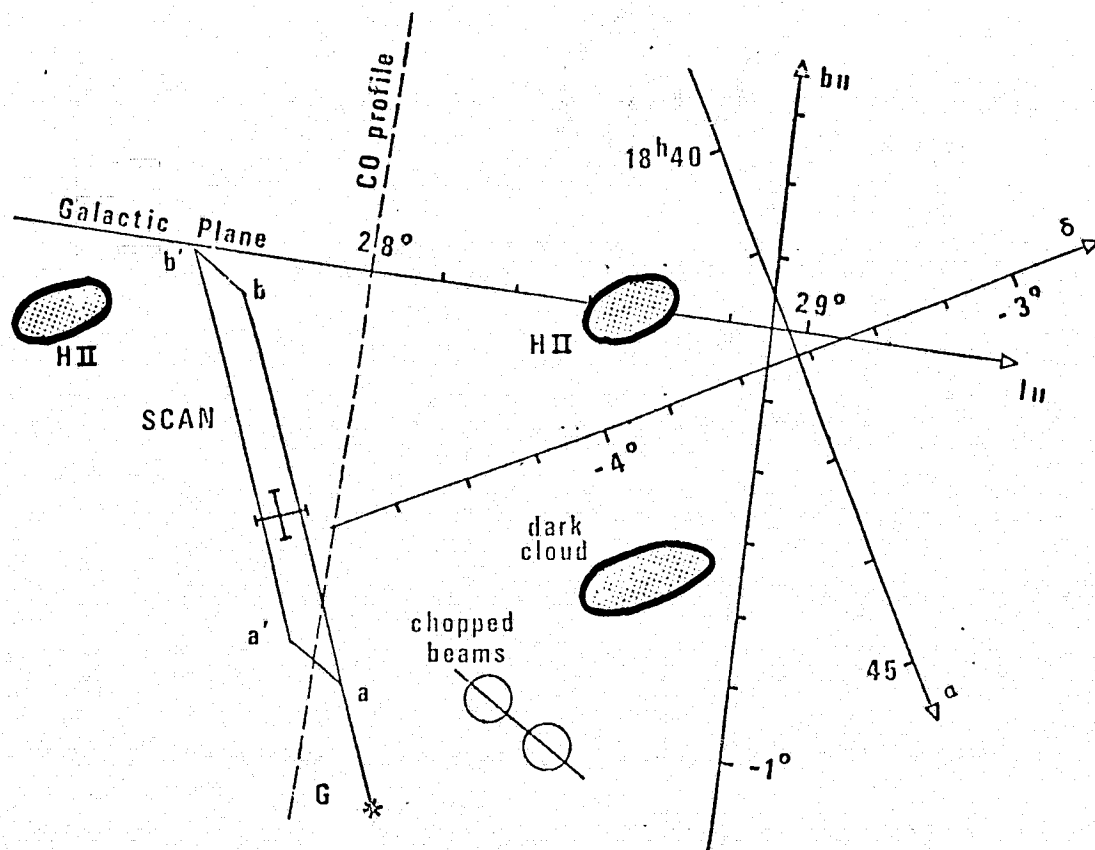


Fig. 1

Orientation of the galactic plane scans. G is the guide star,  $aa'$   $bb'$  the extreme positions of the center of the chopped beams. Gray areas show known sources: HII regions, dark cloud B133.

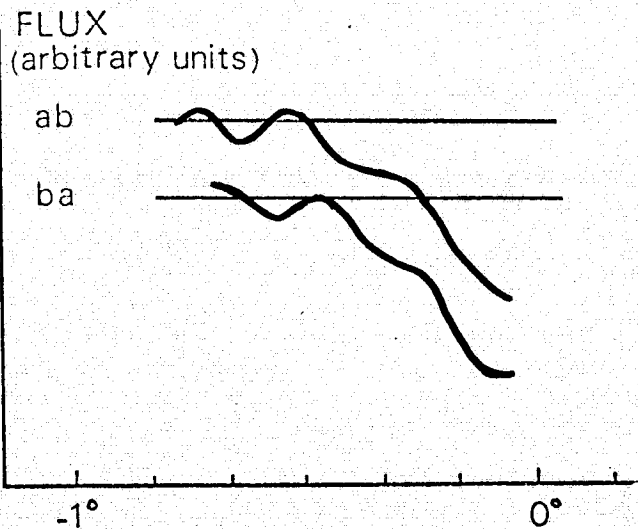


Fig. 2

Averaged scans in directions  $ba$  and  $ab$ .

Discovery of a Far Infrared Source in W45  
with a New Balloon-Borne Helium-Cooled .4-meter Telescope

M. F. Campbell, P. M. Harvey, W. F. Hoffmann, University of Arizona; M. R. Jacobson, D. B. Ward\*, M. O. Harwit, Cornell University (\*now at University of Groningen); P. A. Aannestad, Arizona State University

On August 5, 1976, a new 0.4-meter, balloon-borne liquid helium-cooled, multichannel far infrared telescope made its first flight from the National Scientific Balloon Facility in Palestine, Texas. It achieved a sky background limited performance with a far infrared photoconductive detector at 100 microns at an altitude of 100,000 feet. The initial survey sensitivity was 150 Janskys per  $\sqrt{\text{Hz}}$ . A small portion of the sky was surveyed with a 12' beam, including a few square degrees along the galactic plane. Accurate determination of positions was made possible by a photometer, sensitive between .4 and 1.0 $\mu$ , at the focus of a 10-cm Newtonian reflector, boresighted to the main telescope. By detecting and identifying stars as faint as eighth magnitude, we computed scan trajectories accurate to 5' of arc azimuth and 7' of arc in elevation. Our data analysis disclosed strong signals at 100 $\mu$  on three consecutive scans at the same sky position, corresponding to the radio source W45.

The telescope, measured 2770 Jy on the central scan at  $18^{\text{h}}53^{\text{m}}.0 \pm 0^{\text{m}}.3$ ,  $+7^{\circ}48' \pm 7'$ . The calibration is based on a retractable black body operated during flight. This calibration is consistent with a subsequent 100 $\mu$  measurement of W45 from the NASA Kuiper Airborne Observatory. In Westerhout's<sup>1</sup> survey of the plane at 1.39 MHz in 1958, the region labeled 45 is a faint extension of the plane, covering  $\sim 2^{\circ}$  in galactic latitude and  $0.8^{\circ}$  in galactic longitude, with a slight central peak. Later measurements by Altenhoff, et al<sup>2</sup> assigned the central peak a diameter of 10' of arc and peak flux densities of 5 and 4 Jy at 1.4 and 5.0 GHz, respectively. Quite recently, Price and Graf<sup>3</sup>, observed a peak flux of 2.4 Jy at 10.7 GHz in a region about 2' of arc wide in R. A., with a hint of structure — two components separated by .7' of arc in R. A. The AFCRL survey<sup>4</sup> denotes the source as 2284, with 435 Jy at 20 $\mu$  and 103 Jy at 11 $\mu$ . Finally, the Sharpless HII region 76, with a diameter of 7' of arc, is in the region.

Analysis of the data for additional sources is underway.

---

<sup>1</sup>Westerhout, G., 1958, B.A.N., 14, 215.

<sup>2</sup>Altenhoff, W. J., Downes, D., Goad, L., Maxwell, A., Rinehart, R., 1970, Astr. Astrophys. Suppl., 1, 319.

<sup>3</sup>Graf, W., Price, K. M., 1976, private communication.

<sup>4</sup>Walker, R. G., Price, S. D., 1975, AFCRL=TR-75-0373.

Fabry-Perot Observations of the SIII,  $^1D_2-^3P_1$  Transition,  
at 9069 Å in the Orion nebula.

H. Olthof

Max-Planck-Institut für extraterrestrische Physik  
8046 Garching, W.-Germany

C. B. Cosmovici

Instituto di Fisica, Università di Lecce, Italy

Abstract

Ionic forbidden line emission resulting from magnetic dipole transitions in the ground state are an important tool to study the density, temperature and abundance structure. In particular for regions, which are obscured by large amount of absorbing material the infrared observations provide the only way to derive abundances.

For SIII the important lines in the infrared originate from the  $^1D_2$  (9069, 9534 Å), the  $^3P_2$  (18.7 μ) and the  $^3P_1$  (33.6 μ) levels. Recently, Baluteau et al. (1976) have reported the detection of the 18.7 μ line in the Orion nebula. During the nights of 9 and 10 October 1976 we have studied the 9069 Å line at different positions in the Orion nebula. For this purpose a tilting Fabry-Perot interferometer was mounted at the Cassegrain focus of the 182 cm telescope of the university of Padua at Cima Ekar (Asiago). The details about this instrument are given by Barbieri et al. (1974, 1976). A blocking filter with width of about 20 Å around 9070 Å was used to isolate the Fabry Perot transmission peak, which by means of tilting in a parallel beam scans the spectral region between 9080 and 9060 Å. The width of the Fabry Perot filter for vertical incidence is 0.7 Å. The tilt of the filter causes a decrease of transmission accompanied by a broadening of the beam width. The total area under the transmission profile remains practically constant (Eather and Reasoner, 1969). During our observations we have used a beam of 38 arc sec.

In a similar way as described by Barbieri et al. (1976) we have calibrated the system by observing standard stars and derived a relation between the I magnitude and the count rate of our SSR photon counter connected to a cooled Ga-As photomultiplier. Although we have measured several positions in the nebula, we will here concentrate on the brightest part which is located one beamsize in the western direction next to the trapezium. In this beam we have observed a radiance of  $2.1 \times 10^{-10} \text{ W cm}^{-2} \text{ sr}^{-1}$  averaged over our 38" beam. This is at least one order of magnitude less than has been predicted (Olthof, 1975).

Three effects may play a role here. In the first place we did not correct internal absorption at this wavelength. However, according to Costero and Peimbert (1971) we would not expect this to have an effect of much more than a factor 2. In the second place the sulphur abundance may be overestimated in the theoretical estimates. A similar suspicion has been put forward by Baluteau et al. (1976). In the third place SIII may not be the most important stage of ionization of sulphur. If large amounts of SIV are present, observations at  $10.5 \mu$  could bring clarification.

### References

- Baluteau, J.P., et al., 1976, symp. on infrared astronomy, XIXth Cospar meeting, Philadelphia.
- Barbieri, C., et al., 1974, *Icarus* 23, 568;  
 " 1976, *Astron. and Astroph.* 47, 255.
- Costero, R., Peimbert, M., *Boll. Tonazintla* 7, 229.
- Eather, R.H., Reasoner, P.L., *Appl. Optics* 8, 227.
- Olthof, H., 1975, thesis, univ. of Groningen, Netherlands.

## High Resolution Mapping of the Orion Nebula Region at 30, 50, and 100 Microns.

M. W. Werner, E. E. Becklin, I. Gatley, and G. Neugebauer, Caltech.

The central  $\sim 4' \times 4'$  region of the Orion Nebula-OMC1 complex has been mapped with  $20''$  resolution in well-defined bands at 30, 50 and  $100 \mu$  from the NASA C-141 infrared observatory. These data provide detailed information about the distribution of matter, luminosity, and temperature in this region. The principal results are the following: A) At all three wavelengths, the surface brightness peaks sharply at the position of the infrared cluster, which includes the Becklin-Neugebauer and Kleinmann-Low objects, to the northwest of the Trapezium. The total 25 to  $130 \mu$  luminosity from a  $30''$  region centered on this peak is  $4 \times 10^4 L_{\odot}$ . B) This emission peak is resolved spatially at all three wavelengths, with a characteristic half-width of  $35''$ . C) The color temperature of the emission at the peak is  $\sim 120$  K. The temperature decreases uniformly away from this peak as expected for a dust cloud heated by a central luminosity source. D) At all three wavelengths, the surface brightness of the emission in the direction of the H II region is measured to be less than 10% of the peak surface brightness. The color temperature of this emission is  $\geq 200$  K. E) At  $50 \mu$  and  $100 \mu$ , there is a strong suggestion of a ring of emission surrounding the H II region, which is well-correlated with the position of optically visible ionization fronts. F) The previously identified bar of emission associated with the ionization front near  $\theta^2$  A Orionis is not resolved at any wavelength and is smaller than  $30''$  in NW-SE extent. G) The total 25- $130 \mu$  emission from the region mapped in  $\sim 2 \times 10^5 L_{\odot}$ . The infrared cluster and the Trapezium cluster appear to make roughly equal contributions to this luminosity.

Far Infrared Lamellar Grating Observations of  
Jupiter and HII Regions.

J.L. Pipher, J.G. Duthie, M.P. Savedoff  
The University of Rochester, Dept. of Physics & Astronomy, Rochester, NY 14627

A lamellar grating interferometer has been used successfully on the Gerard P. Kuiper Airborne Observatory to obtain spectra at wavelengths longer than  $50\mu$  of Jupiter and several HII regions. We have improved the resolution of our Jupiter spectra to  $1.6\text{ cm}^{-1}$ , using the Moon as a standard, and the HII region spectra are all at resolutions of  $13\text{ cm}^{-1}$  (regions well-studied include the Kleinmann-Low Nebula and W51; preliminary data on NGC 7538, DR 21, M 17 and W 3 have been obtained). In our wavelength interval, the main opacity in the Jovian atmosphere is the rotational spectrum of  $\text{NH}_3$  plus the translational continuum due to  $\text{H}_2$ . Theoretical spectra of the Jovian atmosphere are compared against our observations and discussed. The HII region spectra are discussed and compared with models based on comparison of our data with that at other wavelengths.

## MEDIUM RESOLUTION SPECTROSCOPY OF NGC 7027 FROM 16 TO 38 MICRONS

J. McCarthy, W. Forrest and J. R. Houck

Center for Radiophysics and Space Research  
Cornell University  
Ithaca, N.Y.

NGC 7027 was observed on two nights, 1976 May 18-19 and 20-21, using the 36" telescope of the KAO. A medium resolution, two-channel, Helium-cooled grating spectrometer was used to observe the bands, 16-23 $\mu$  ( $\Delta\lambda = 0.5\mu$ ) and 20-38 $\mu$  ( $\Delta\lambda = 1.2\mu$ ). A nearly flat smooth continuum over the entire band was observed with a peak intensity of  $7 \times 10^{-16}$  w/cm<sup>2</sup> $\mu$  between 20 and 25 $\mu$ .

The 8-14 $\mu$  spectrum of 7027 has several spectral features. The strongest of these is a broad 11.3 $\mu$  emission band which has been tentatively identified by Gillett as due to carbonate grains. Laboratory measurements of the carbonate grains that are most likely to be abundant, MgCO<sub>3</sub>, CaCO<sub>3</sub> and FeCO<sub>3</sub>, have been made by Angino and Morandat *et al.*, using various suspension and pellet techniques. Penman has calculated the emission coefficient for small grains on the basis of Mie theory and the bulk dielectric coefficients. These investigations predict a longwavelength (22 to 35 $\mu$ ) carbonate lattice resonances, which are in general stronger than the 11.3 $\mu$  resonance. Our spectrum does not show any isolated emission features in the 22 to 35 $\mu$  range. This result will be discussed in terms of a smeared out feature or features and alternate mechanisms for generating the longwavelength continuum.

No evidence of the 25.87 $\mu$  fine structure line of OIV was observed. A three  $\sigma$  upper limit of  $2 \times 10^{-16}$  w/cm<sup>2</sup> is set by our data. Simpson had predicted a flux of  $3.8 \times 10^{-16}$  w/cm<sup>2</sup>. This difference can be reconciled by a slight increase in the assumed electron density. Our spectrum is consistent with  $n_e > 2.5 \times 10^4$  cm<sup>-3</sup>. Scott *et al.*, have derived a value of  $n_e = (5.0 \pm 0.5) \times 10^4$  cm<sup>-3</sup> from high resolution 5 GHz observations.

This work was supported by NASA grant NGR 33-010-081.

Angino, E.E. *Am Mineralogist* 52, 137 (1967).

Morandat, M.J., Lorenzelli, M.V., and Lecomte, J. *Journal de Physique* 28, 152 (1967).

Penman, J.M. Preprint.

4-8  $\mu$  Spectrophotometric Observations of NGC 7027 and M82R. W. Russell, B. T. Soifer, and S. P. WillnerDepartment of Physics  
University of California, San Diego

## ABSTRACT

4-8  $\mu$  spectrophotometry of the planetary nebula NGC 7027 and of the nucleus of the galaxy M82 is presented. The data were obtained with the Kuiper Airborne Observatory and the UCSD liquid nitrogen-cooled filter wheel spectrometer with a resolution  $\Delta\lambda/\lambda$  of 0.015, utilizing an arsenic-doped silicon photoconductive detector operated at 4 K. All phases of the spectrometer control and data acquisition, processing, and real-time display were accomplished by the onboard Data Acquisition System, under interactive control by the observers. The observations were made with a 30'' aperture and a 2' beam separation. From an altitude of  $\sim 12.5$  km, there was about  $6.5 \mu$  of residual water vapor along the line of sight. Data reduction and first order corrections for telluric absorptions were accomplished by comparison with observations of the standard star  $\alpha$  Boo.

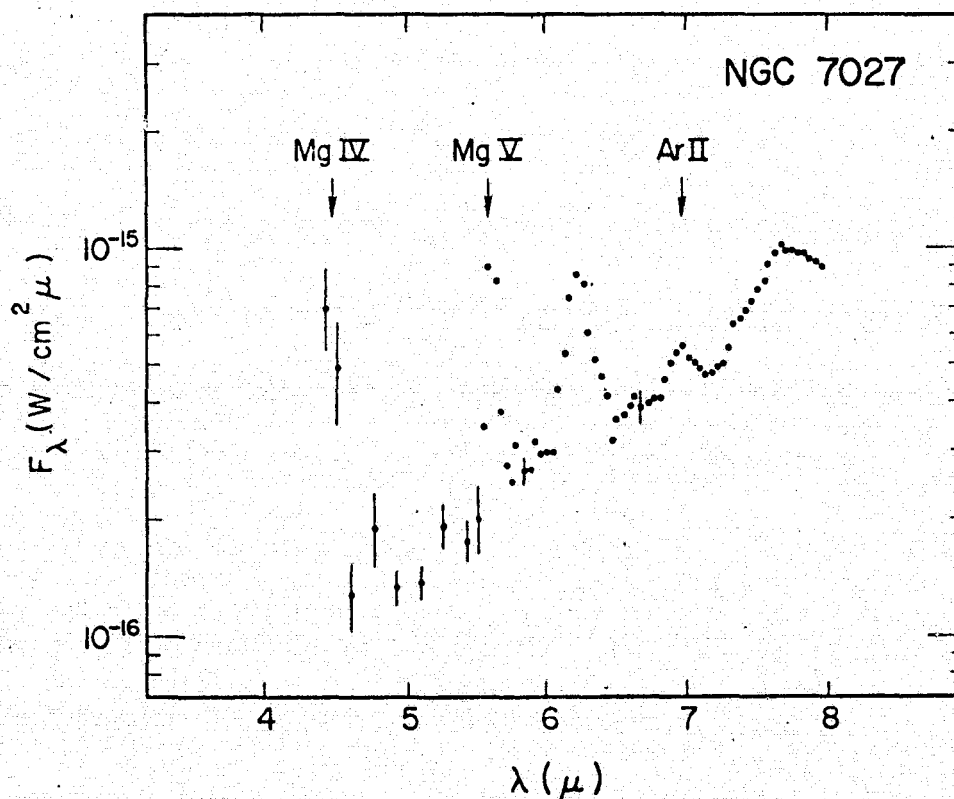


Fig. 1. The 4-8  $\mu$  spectrum of NGC 7027. Identified fine structure lines of Mg IV, Mg V, and Ar II are noted.

The data on NGC 7027 are displayed in Fig. 1, where the following identifications of atomic lines are marked: Mg IV at 4.49  $\mu$ , Mg V at 5.61  $\mu$ , and Ar II at 6.98  $\mu$ . In addition to these identified features, there is a new feature at 6.23  $\mu$  which is broader than the instrumental resolution. All of these features are superimposed on a continuum which is an order of magnitude above the expected level of free-free radiation. The continuum rises steadily to a broad peak at about 7.7  $\mu$ .

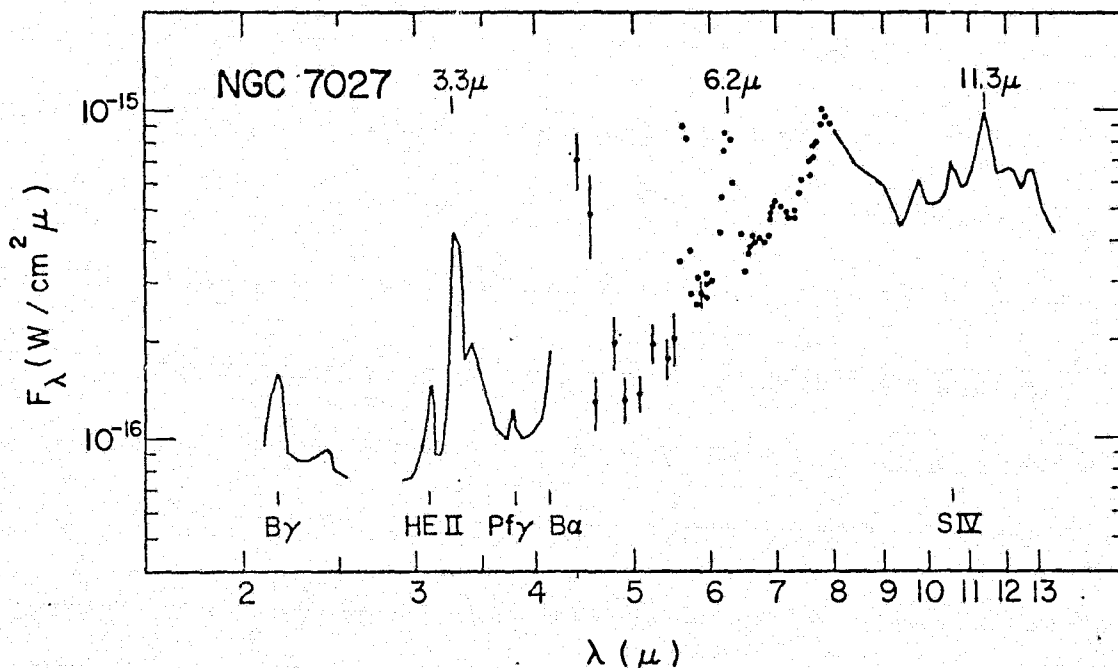


Fig. 2. The 2-13  $\mu$  spectrum of NGC 7027. Atomic transitions and possible dust emission features are noted.

From Fig. 2, where we have included ground-based data from 2-4  $\mu$  (Merrill, Soifer, and Russell 1975) and from 8-14  $\mu$  (Gillett, Forrest and Merrill 1973), one can see that the 7.7  $\mu$  peak is too narrow for a single black body distribution. If the infrared continuum is due to emission from dust, as is generally accepted, the 7.7  $\mu$  feature should be attributed to a peak in the emissivity of the dust. Gillett *et al.* (1973) have proposed carbonates as possible constituents of the dust, based on the presence of an 11.3  $\mu$  emission feature seen in their data as reproduced in Fig. 2. Because terrestrial carbonates show an even larger peak in their emissivity (Hunt, Wisherd, and Bonham 1950) at 7  $\mu$  than at 11.3  $\mu$ , it would appear that either carbonates are not responsible for the 11.3  $\mu$  feature or, if they are, the wavelength of peak emission is shifted (possibly due to compositional differences between the material in NGC 7027 and the comparison materials).

The 6.2  $\mu$  emission feature is broader than the instrumental resolution, and is therefore either a combination of atomic lines, a molecular band, or a solid particle resonance feature. The same 6.2  $\mu$  feature was detected in the

spectrum of the galaxy M82. Since the excitation conditions in the two nebulae are drastically different, the simplest interpretation is that the feature is due to solid particle emission.

Emission features at  $3.3 \mu$  and  $11.3 \mu$ , as well as that at  $6.2 \mu$ , are observed in both NGC 7027 and M82. The ratios of their strengths (after correcting for the large extinction to the nucleus of M82) are the same in both objects, supporting the view that they are emission features in the dust.

The atomic lines seen in Figs. 1 and 2 are particularly useful in analyzing the properties of the central star and the nebular ionic abundances. In particular, Mg V represents the highest ionic state thus far identified in NGC 7027. Due to its high ionization potential (109.3 eV), the intensity of the Mg V line is sensitive to the temperature of the central star. Assuming that all uv photons with an energy greater than 109 eV are absorbed by Mg IV ions, and the stellar luminosity is given by the observed infrared luminosity, a lower limit of 125,000 K is determined for the temperature of the central star. In fact, oxygen is probably a significant competitor for the uv flux, and a correction to the uv flux estimate of a factor of 25, the cosmic abundance ratio of oxygen to magnesium, results in  $T_{\text{star}} \sim 200,000$  K. This can be regarded as a crude upper limit to the stellar temperature.

Ionic abundances can be calculated from the intensities of the various infrared lines. Such abundances are particularly useful as there is negligible reddening at these wavelengths, and, for the ions considered here, the line strengths are only weakly dependent upon the temperature and density. The observed ratio  $n(\text{Mg V})/n(\text{H II})$  is  $1.7 \times 10^{-5}$ , or 0.6 of the normal cosmic Mg abundance. The relative ionic abundances as a function of ionization potential deduced from optical observations (Kaler *et al.* 1976) suggest that there should be much more Mg IV than Mg V. It thus appears that Mg is considerably overabundant in NGC 7027. The observed Mg IV line at  $4.49 \mu$  is much weaker than expected, probably owing to a wavelength coincidence with a narrow telluric absorption line.

ACKNOWLEDGEMENTS -- We would like to thank P. Brissenden for technical assistance, K. Sellgren for assistance with the observations, and R. Puetter for assistance with the data reduction. Airborne Infrared Astronomy at UCSD is supported by NASA grant NGR 05-005-055.

#### REFERENCES

- Gillett, F. C., Forrest, W. J., and Merrill, K. M. 1973, Ap. J. 183, 87.  
 Hunt, J. M., Wisherd, M. P., and Bonham, L. C. 1950, Anal. Chem. 22, 1478.  
 Kaler, J. B., Aller, L. H., Czyzak, S. J., and Epps, H. W. 1976, Ap. J. Supp. 31, 163.  
 Merrill, K. M., Soifer, B. T., and Russell, R. W. 1975, Ap. J. (Letters) 200, L37.

## ORIGIN OF 40-350 MICRON FLUX IN SOURCES ASSOCIATED WITH HII REGIONS.

J.P. EMERSON

Department of Physics and Astronomy  
University College London  
Gower Street  
LONDON WC1E6BT  
ENGLAND

The 40-350 micron photometric observations (obtained with the UCL 40 cm balloon borne telescope) of almost fifty sources associated with HII regions are used to investigate the location, composition and temperature of the emitting dust. The possible locations considered are inside HII regions and inside the surrounding molecular clouds.

Comparison of infrared and radio observations with fluxes predicted from model stellar atmospheres indicates that there is dust inside the HII regions with an optical depth for absorption of Lyman continuum photons of about one. This is broadly consistent with gas to dust ratios about equal to that in the interstellar medium, although some details are unclear and will be discussed.

The temperatures of ice (or ice covered cores), silicate and graphite grains which are required to explain the 40-350 micron emission as arising from dust mixed with gas, in the same ratio as in the interstellar medium, are evaluated using gas masses derived from radio continuum observations in the case of HII regions, and from the formaldehyde absorption line in the case of molecular clouds. This approach minimises the dependence of the output parameter on the input parameters.

The temperatures derived are compared with temperatures derived from multi-band photometric observations. Graphite grains have too low an emissivity to produce the emission from either location. Ice grains (or ice mantles) in HII regions ( $T \approx 80$  K) best match the multiband results. Ice in molecular clouds would have to be at about 40 K and silicates at about 60 K, both lower than suggested by the multiband results.

The similarity of radio and far infrared positions and maps also suggests dust in the HII regions.

It is concluded that the majority of the radiation from the 40-350 micron objects associated with HII regions can be attributed to thermal emission from ice grains (or ice mantles) at about 80 K mixed with ionized gas and with a gas to dust ratio similar to that in the interstellar medium. No indication is found, for these objects, of a substantial contribution (compared to that from the HII region) to the flux from molecular clouds.

---

INFRARED EMISSION AND PROPERTIES  
OF DUST OF GASEOUS NEBULA

Vahé Petrosian and Roger A. Dana  
Institute for Plasma Research  
Stanford University

and

L. J. Caroff  
NASA-AMES Research Center

The infrared emission from HII regions and other nebulae provides useful information on the properties of dust grains associated with these nebulae. It is the purpose of this report to present simple analytic results from radiative transfer in dusty nebula which relate the observational characteristics (such as the infrared to optical and radio flux ratios, the gas density, infrared spectrum and half-power angular sizes at various wavelengths) to physical parameters such as dust-to-gas ratio, infrared and optical opacity of the grains, and the gas and dust distributions, etc.

These relationships will be presented and the extent that they can be useful for the determination of physical parameters will be discussed.

A statistical analysis of the data on the infrared emission of galactic and extragalactic HII regions has been carried out. The results show that because of the existence of many independent variables it is difficult to draw a definite conclusion on the properties of dust grains except for sources with well known spectra taken over a wide range of wavelengths.

The particular problem which we shall address is the meaning of the presence or absence of a correlation between infrared and radio flux densities (DeJong, et al 1975, Felli, et al 1974, Kazes, et al 1975, Mezger and Henderson 1967, Schraml and Mezger 1969, Shaver and Gross 1970, and Walker and Price 1975) and the low level of observed infrared fluxes from extragalactic HII regions (Strom, et al 1974).

This work was partially supported by the NASA-AMES University Interchange Agreement NCA2-OR745-613.

## REFERENCES

- DeJong, T., Israel, F. P. and Tielens, A.G.G.M. 1975, HII Regions and Related Topics, (Proceedings of a Symposium Held at Mittelberg, Kleinwalsertal, Austria, January 13-17) Eds: T. L. Wilson and D. Downes, (Berlin: Springer-Verlag). p. 123.
- Felli, M., Tofani, G., and D'Addario, L. R. 1974, *Astron. and Astrophys.* 31, 431.
- Kazés, I., Lesquères, A.M. and Gadéa, F. 1975, *Astron. and Astrophys.* 42, 9.
- Mezger, P. G. and Henderson, A. P., 1967, *Ap. J.* 147, 471.
- Schraml, J. and Mezger, P. G. 1969, *Ap. J.* 156, 269.
- Shaver, P. A. and Gross, W. M. 1970, *Aust. J. Phys. Astronophys. Suppl.* 14, 133.
- Strom, S. E., Strom, K. M., Grasdalen, G. L. and Capps, R. W. 1974, *Ap. J. Letters*, 193, L7.
- Walker, R. G. and Price, S. D. 1975, AFCRL-TR-75-0373.

ON THE ENERGY BALANCE OF THE INFRARED RADIATION IN  
PLANETARY NEBULAE, GALACTIC AND EXTRAGALACTIC H II REGIONS

K.V.K. Iyengar and K.S. Krishna Swamy  
Tata Institute of Fundamental Research  
Homi Bhabha Road, Bombay 400005, India

ABSTRACT

Most of the planetary nebulae, galactic and extragalactic H II regions emit lot of infrared radiation over and above the free-free emission from the ionized gas. It is generally believed that this excess of observed infrared radiation arises from the thermal re-radiation by the dust grains. The energy input to the grain ultimately has to come from the central star. In these nebulae considerable portion of the stellar energy is converted into the emission lines and Ly  $\alpha$  ( $\text{Ly } \alpha$ ) radiation. Therefore it is reasonable to assume that the heating of the grain arises mainly from the absorption of these Ly  $\alpha$  photons. If this is the heating mechanism of the grain, then one expects a linear relation between the radio flux and the infrared flux. In the present paper, we present calculations on the expected relation between the radio flux and the infrared flux based on the particle models and Ly  $\alpha$  heating mechanism. These are then compared with the observed relation for the three types of objects.

The model and the method of calculation are essentially those of Krishna Swamy and O'Dell (1968) and Krishna Swamy (1969). The Ly  $\alpha$  flux is calculated from a knowledge of the radio flux. Since the composition of the grains in these nebulae is still far from clear, we perform the calculations for two types of possible grain models, namely, graphite and silicate. For silicate model, we have used as representative the results for two rocks viz. 14321 and 12009 of Apollo samples (Perry et al. 1972). The calculations are performed for typical graphite and silicate grains of radii 0.02 and 0.2  $\mu$  respectively. We have used an electron temperature of 12,000 $^{\circ}$ K for all planetary nebulae and 10,000 $^{\circ}$ K for all galactic and extragalactic H II regions.

For planetaries, we have calculated the expected infrared fluxes using the radio flux at 10GHz (Higgs 1971). Since Cohen and Barlow (1974) have given their infrared observations in terms of absolute magnitudes, we have converted our calculated infrared fluxes to absolute magnitudes using their tabulated distances and the calibration. In Figures 1 and 2, we show a comparison of the observed and the calculated absolute magnitudes at 10 and 18  $\mu$  for the graphite model. The results are shown for two values of  $F(\cong 3f)$  equal to 1 and 30. Here  $f$  represents the path length of Ly  $\alpha$  photons (O'Dell 1965) whose value lies roughly in the range 1 to 30 (Capriotti 1967). As can be seen from these figures that the agreement is quite good. This means that the Ly  $\alpha$  heating of the grain is sufficient to explain the observed infrared radiation from planetary nebulae. It is also found that the observations fit better with the graphite model than with the silicate model and that the grains are present in the ionized region. The ratio of dust to gas (Md/Mg) for the graphite model lies roughly in the range  $10^{-1}$  to  $10^{-4}$ .

For Galactic H II regions, the calculated infrared fluxes were always found to be smaller than those of observations for both the graphite and silicate models. Therefore, we introduced a parameter  $M$ , a factor by

which the Ly  $\alpha$  flux is to be increased to bring an agreement with the observations. In Figures 3 and 4, we have compared the expected relation between the radio flux at 11 cm (Altenhoff et al. 1970) and the infrared flux at 11 and 20  $\mu$  for different values of M with F equal to 30 for the graphite model, with the observed relation of Strom et al. (1974). To get an agreement between the calculations and observations, one requires  $M \approx 3$  to 5. This is consistent with other investigations based on the total infrared luminosity. The extra flux has to come from the direct absorption of the ionizing stellar continuum. However, at the present time, it is very hard to construct a meaningful physical model as there are too many variable parameters connected with the model grains: Such as the type of grains, single, mixture or composite type and their composition, their size distribution function, the wavelength dependence of their refractive index etc. Hopefully such a calculation will be feasible, when more information becomes available of the physical and chemical nature of grains present in the HII regions.

Using  $M = 5$  and  $F = 30$ , which gave a good fit for the Galactic HII regions, we have calculated the expected relation between the radio flux (Israel and Van der Kruit 1974) and the infrared flux for extragalactic HII regions. These are compared with the few available infrared observations of extragalactic HII regions of Strom et al. (1974). It is shown that their infrared observations are consistent with the expected infrared fluxes for these objects.

#### References:

- Altenhoff, W.J., Downes, D., Goad, L., Maxwell, A. and Rinehout, R. 1970, Astr. and Ap. Suppl., 1, 319.
- Capriotti, E.R., 1967, Ap. J., 150, 79.
- Cohen, M. and Barlow, M.J., 1974, Ap. J., 193, 401.
- Higgs, L.A., 1971, Catalog of Radio Observations of Planetary Nebulae and Related Optical Data (Pub. Ap. Branch, N.R.C., Canada), Vol. 1, No. 1.
- Israel, F. and van der Kruit, P.C., 1974, Astr. and Ap., 32, 363.
- Krishna Swamy, K.S. and O'Dell, C.R. 1968, Ap. J., 151, L61.
- Krishna Swamy, K.S. 1969, P.A.S.P., 81, 154.
- O'Dell, C.R. 1965, Ap. J., 182, 503.
- Perry, C.H., Agrawal, D.K., Anastassakis, E., Lowndes, R.P., Rastogi, A. and Tornberg, N.E. 1972, Moon, 4, 315.
- Strom, S.E., Strom, E.M., and Grasdalen, G.L., 1974, Ap. J., 193, L7.

Captions

- Fig. 1 Comparison of the observed and calculated absolute magnitudes at  $10\mu$  for the graphite model for  $F = 1$ (a) and  $F = 30$  (b) respectively.
- Fig. 2 Same as Fig. <sup>but</sup>  $1_{\mu}$  for  $18\mu$ .
- Fig. 3 Comparison of the Radio flux at 11 cm versus  $m(11\mu)$  for graphite model with  $F = 30$ .  $M = 3$  ( $\square$ ),  $M = 7$  ( $\blacktriangle$ ) and observations ( $\bullet$ ). The line shown in the figure is that drawn by Strom et al. to pass through the observational points.
- Fig. 4 Same as Fig. 3, but for  $20\mu$ .  $M = 1$  ( $\blacktriangle$ ),  $M = 3$  ( $\square$ ),  $M = 7$  ( $\blacklozenge$ ) and observations ( $\circ$ ).

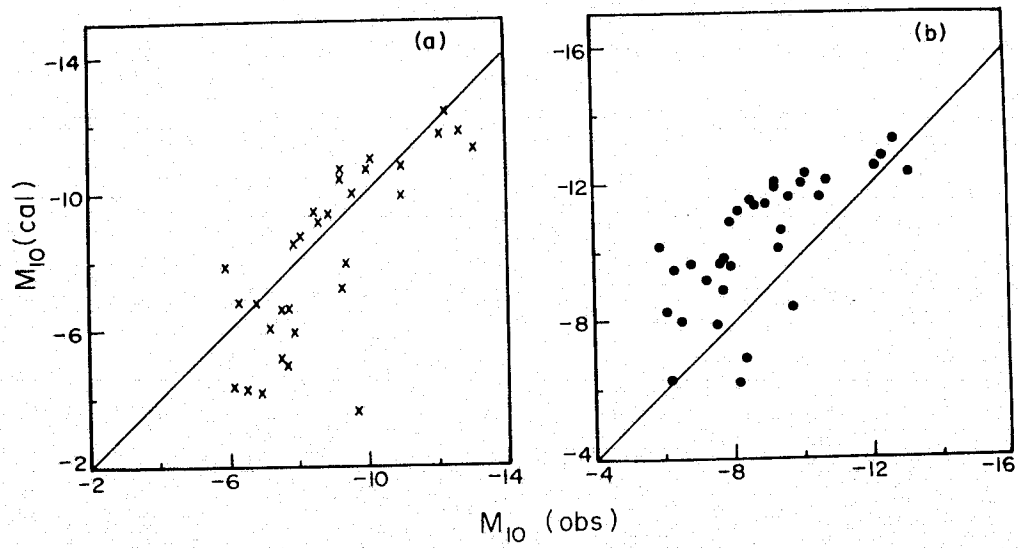


Fig. 1

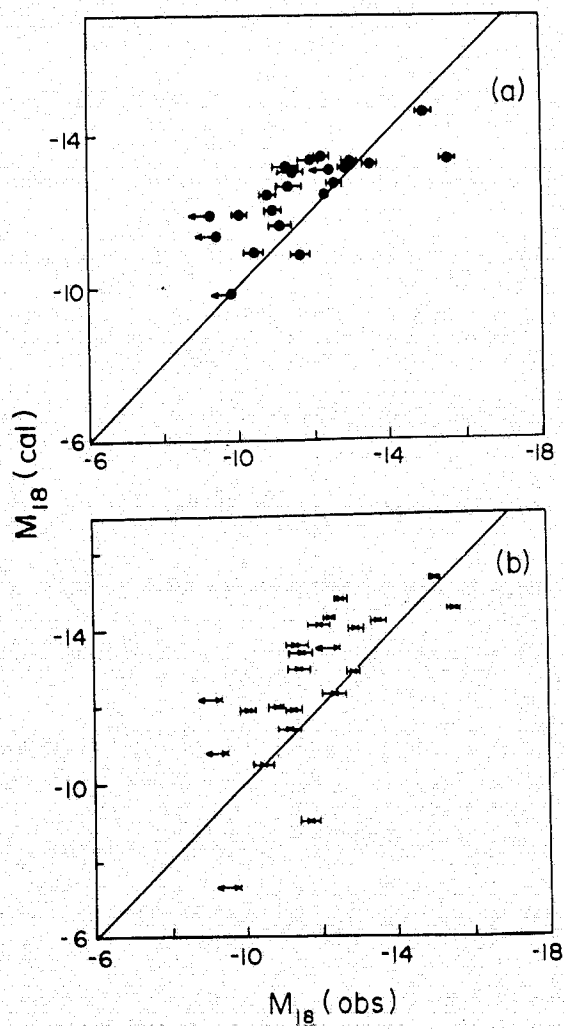


Fig. 2

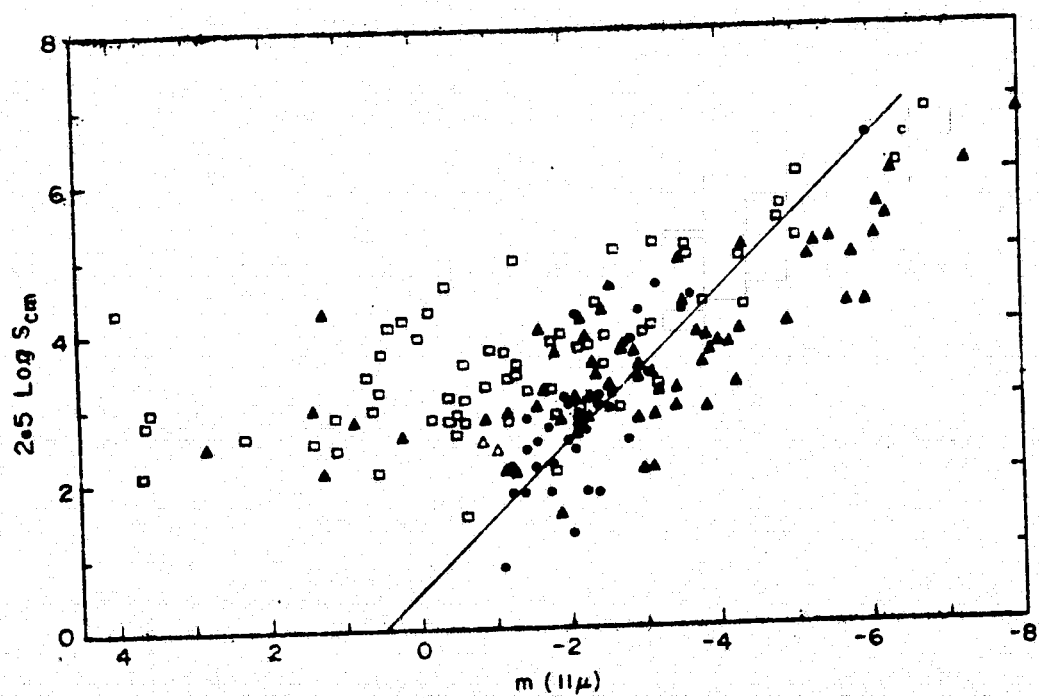


FIG. 3

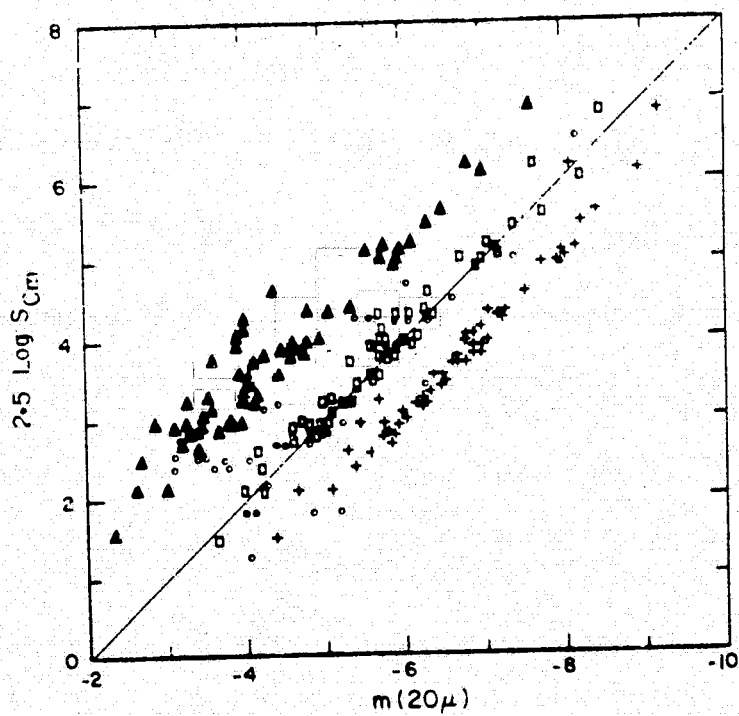


FIG. 4

IV. GALAXIES

## Airborne Far Infrared Observations of the Galactic Center Region.

I. Gatley, E. E. Becklin, M. W. Werner, and C. G. Wynn-Williams, Caltech.

Maps of a region 10' in diameter around the galactic center made from the NASA Kuiper Airborne Observatory simultaneously in three wavelength bands at 30  $\mu$ , 50  $\mu$ , and 100  $\mu$  with  $\sim 1'$  resolution are presented, and the distribution of far infrared luminosity and color temperature across this region is derived. The position of highest far infrared surface brightness coincides with the peak of the late-type stellar distribution and with the H II region Sgr A West. The high spatial and temperature resolution of the data is used to identify features of the far infrared maps with known sources of near infrared, radio continuum, and molecular emission. The emission mechanism and energy sources for the far infrared radiation are analyzed qualitatively, and it is concluded that all of the observed far infrared radiation from the galactic center region can be attributed to thermal emission from dust heated both by the late-type stars and by the ultraviolet sources which ionize the H II regions. A self-consistent model for the far infrared emission from the galactic center region is presented. It is found that the visual extinction across the central 10 pc of the Galaxy is only about 3 magnitudes, and that the dust density is fairly uniform in this region. The absorption efficiency of the grains is found to vary as  $\lambda^{-1}$  out to 100  $\mu$ . An upper limit of  $10^7 L_{\odot}$  is set on the luminosity of any presently unidentified source of 0.1 to 1  $\mu$  radiation at the galactic center.

PRELIMINARY RESULTS OF A BALLOON-BORNE OBSERVATION OF THE FAR INFRA-RED GALACTIC DIFFUSE EMISSION BETWEEN  $l=38^\circ$  AND  $l=55^\circ$ .- G. SERRA (Centre d'Etudes Spatiales des Rayonnements, Toulouse, France), J.L. PUGET (Observatoire de Paris-Meudon, Meudon, France), and C. RYTER (Centre d'Etudes Nucleaires de Saclay, Gif sur Yvette, France).

A far infra-red instrument operating in the bands  $\lambda=75-95 \mu\text{m}$  and  $\lambda=115-196 \mu\text{m}$  has been designed to detect low brightness extended sources. Given the characteristics of the bolometers, a field of view of  $\sim 0.7^\circ$  is required to achieve the required sensitivity.<sup>1</sup> The orientation of the gondola is locked on the Earth magnetic field, at an angle adjustable by telecommand. The altitude angle of the telescope (with respect to the vertical) is set before the flight. The azimuth angle is swung  $\pm 10^\circ$  with respect to the reference azimuth at a frequency  $\sim 0.2 \text{ sec}^{-1}$ . In this way, a zone  $\leq 20^\circ$  wide is progressively covered in the sky by the rotation of the Earth, with an increment  $0.02^\circ$  between scans.

The instrument was launched on Sep. 23, 1976, from Aire-sur-Adour, France, and reached ceiling altitude at 2115 UT. The galactic plane was continuously observed between  $l=38^\circ$  and  $l=55^\circ$ , in scans oriented at an angle  $75-80^\circ$  with respect to it. We report here some results of a preliminary analysis of the data obtained in the long wavelength range,  $\lambda=115$  to  $\lambda=196 \mu\text{m}$ .

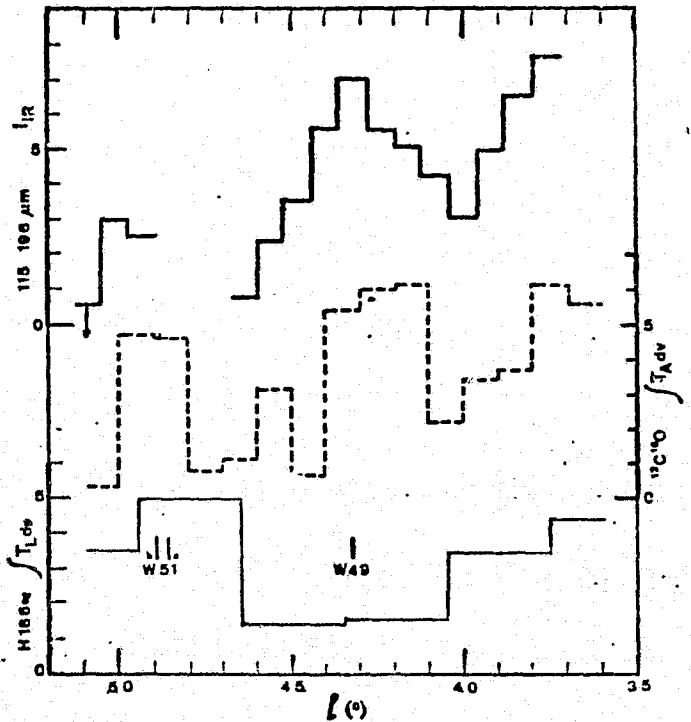
The signal produced by the galactic plane emission is detectable by eye in most of the survey by summing up 16 scans in a "stack". The drift during such an elementary observation due to the rotation of the Earth is  $\sim 0.3^\circ$ , compatible with the angular resolution. Averages over four such stacks, representing five minutes of observation, are displayed in figure 1 as the solid line. They represent the  $115-196 \mu\text{m}$  brightness,  $I_{\text{IR}}$ , at  $b=0$ .

It is evident from the picture that far IR emission takes place quite continuously over the galactic plane in the surveyed area, giving further support to the observations of a diffuse IR emission at  $l=2.5^\circ$  (Pipher 1973), at  $l=0-15^\circ$  (Low 1976), and at  $l=29^\circ$  (Rouan et al. 1976). The prominent HII regions W49 and W51 cannot account by themselves for the observed distribution. Furthermore, the longitude distribution of ionized hydrogen, represented by the light line (Lockman 1976), is not reflected by the IR distribution. Finally, if the radiation in the long wavelength band were largely contributed by dust at the temperature  $t \approx 70^\circ$  usual in HII regions, the total radiated power would be prohibitively high.

The direct observation of a diffuse galactic far IR emission is no unexpected finding. Puget et al. (1976) and Ryter and Puget (1976) have shown that several unrelated observations did point to the existence of a strong diffuse galactic emission produced by the dense interstellar medium, as it is traced by the carbon monoxide (CO) 2.2 mm emission. Indeed, it can be shown that the dust able

<sup>1</sup>The two-channel detector was kindly supplied by the Space Research Laboratory, Rijks University (Groningen, Holland), by courtesy of Professor R.J. van Duinen and Dr J.J. Wijnbergen.

Figure 1.- Observed far IR emission,  $I_{IR}$ , of the galactic plane in the 115-196  $\mu\text{m}$  band, as a function of the galactic longitude. The total  $^{12}\text{C}^{16}\text{O}$  antenna temperature (dotted line, Burton 1976), and the total H 166 antenna temperature (light line, Lockman 1976), are given for comparison. All quantities are in arbitrary units. Note that the galactic far IR emission is not dominated by the H-II regions W49 and W51, and that it exhibits some correlation with the CO distribution.



to heat the molecular clouds at the temperatures observed in the CO line may be detected by its own far IR radiation.

The antenna temperature of the  $^{12}\text{C}^{16}\text{O}$  emission (taken from Burton 1976, averaged over  $1^\circ$  bins) is displayed in figure 1 as the dotted line. Some correlation with the far IR radiation profile is evident, and quantitative estimates can be made. The far IR radiation of molecular clouds is best expressed as a luminosity normalized per hydrogen atom,  $L_{IR}^H$ , deduced from the comparison of the IR brightness,  $I_{IR}$ , and the matter column density on the line of sight,  $N_H = 2N_{\text{H}_2}$ , as

$$L_{IR}^H = 4 \pi \xi^{-1} I_{IR} / N_H, \quad (1)$$

where  $\xi$  represents the fraction of the power radiated in the 115-196  $\mu\text{m}$  band, and depends on the temperature. Although the final data reduction is not completed at the time of writing, a provisional value of  $L_{IR}^H$  can be quoted, with an error which should not exceed a factor  $2 \sim 3$ . We find

$$\begin{aligned} T = 20 \text{ K} : & \quad L_{IR}^H = 1 \times 10^{-30} \text{ w(H atom)}^{-1} \\ T = 30 \text{ K} : & \quad L_{IR}^H = 2 \times 10^{-30} \text{ " " } \end{aligned} \quad (2)$$

The temperature  $T = 30 \text{ K}$  is a likely upper limit set by the 75-95  $\mu\text{m}$  band, and a temperature significantly below 20 K would be insufficient to even account for the radiation in the long wavelength band.

The values quoted in equation 2 are consistent with those deduced by Ryter and Puget (1976). It can be shown that they are at least one order of magnitude above that could be expected if the dust were

solely heated by the general stellar radiation field. It is necessary that the molecular clouds in general are heated by some powerful mechanism, and the most likely one is the presence of young, still undetectable stars. A star formation rate per unit mass of interstellar gas can be deduced in this way, and it is found to be quite high, perhaps one order of magnitude above the value deduced from star counts in the solar vicinity. The reasons for the discrepancy are not very clear at present, but there is a strong suggestion, arising both from CO observations and from far IR observations, that the star formation rate in the Galaxy may quite higher than usually accepted.

#### References:

- Burton, W.B. 1976, The Structure and Content of the Galaxy and Galactic Gamma Rays, ed. by C. Fichtel and F. Stecker (Symposium held at Goddard Space Flight Center, June 2-4.)
- Lockman, F.J. 1976, Ap. J. 209,429.
- Low, F. 1976, COSPAR Symposium on IR Astronomy (Philadelphia, June 8-11.)
- Pipher, J. 1973, IAU Symposium no 52, Interstellar Dust and Related Topics, ed. by J.M. Greenberg and H.C. van de Hulst (Dordrecht: Reidel).
- Puget, J.L., Ryter, C., and Serra, G. 1976, The Structure and Content of the Galaxy and Galactic Gamma Rays, ed. by C. Fichtel and F. Stecker (Symposium held at Goddard Space Flight Center, June 2-4.)
- Rouan, D., Léna, P., Puget, J.L., and de Boer, K. 1976, submitted to Ap. J. (letters).
- Ryter, C., and Puget, J.L. 1976, submitted to Ap. J.

Infrared Polarimetry of Galactic Nuclei, R. F. Knacke, SUNY, Stony Brook.

Polarization observations of extragalactic sources can provide insights into the nature of the radiation processes in these objects. We are conducting a program of infrared (2-15 $\mu$ ) polarization measurements of the galactic nucleus, external galaxies, and other extragalactic objects; and can now report on results of some of the observations. The instrumentation consists of conventional infrared photometers converted to polarimeters by the addition of wire grid polarizers. At present the observations are limited to the ground-based infrared wavelength region, but they could be extended to the airborne infrared to 50 $\mu$  and possibly beyond with available polarizers.

Galactic Nucleus

The center of the Galaxy (Sgr A) has strong wavelength-dependent polarization between 1 and 14 $\mu$ . Polarization maps of the infrared sources are shown in Figures 1a and 1b, where the polarization strength is proportional to the length of the lines and the orientation gives the direction of the E-vector.

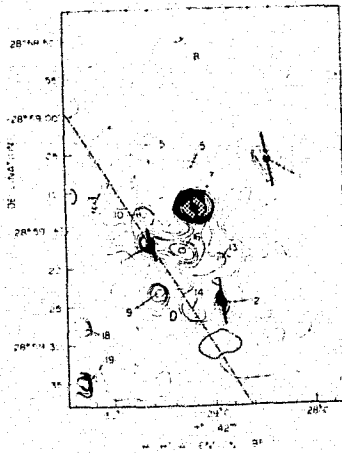


Fig. 1a. 2.2 $\mu$

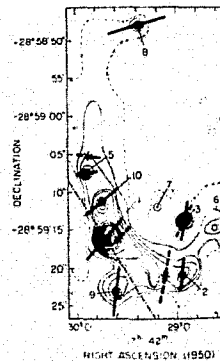
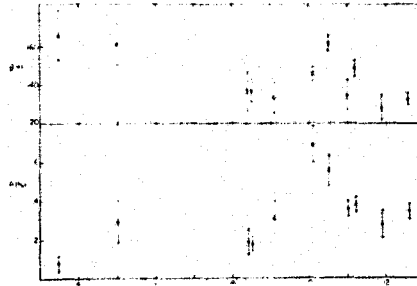


Fig. 1b. 11.5 $\mu$

At 2.2 $\mu$  the polarization direction is nearly parallel to the direction of the galactic plane (shown as the dash-dot line). Since this is also parallel to the predominant direction of visible polarization by interstellar grains, we believe that the 2.2 $\mu$  polarization is also due to grains in the spiral arms. At 11.5 $\mu$  the direction is predominantly perpendicular to the plane, although it varies across the infrared sources. This polarization probably originates in or near the infrared objects at the galactic center.

The polarization is largest in the "silicate" feature at 9.8 $\mu$ ; the polarization-wavelength curve (Figure 2) looks like the (inverted) silicate absorption feature in Sgr A. This shows that the polarization is caused by aligned silicate grains.



At the hydrogen density of order  $10^4 \text{ cm}^{-3}$ , determined from CO observations of Sgr A, a field of order  $10^{-3}$  gauss is required to give the infrared polarization from Davis-Greenstein alignment. More efficient alignment mechanisms could reduce the required magnetic field.

A limit on the  $9.8\mu$  absorption strength can be derived from the wavelength dependence of the ratio of polarization to optical depth. We find  $K_{9.8\mu} < 3 \times 10^3 \text{ cm}^2 \text{ g}^{-1}$ , in rough agreement with the  $K$  derived from polarization in the KL nebula and from spectroscopy of HII regions. This  $K$  shows that the absorption strength is weaker than in most terrestrial silicates or that the silicate is contained in a matrix of other material. The grain silicate may resemble carbonaceous chondrite minerals or an amorphous silicate recently studied by Day (Ap.J., in press).

The  $2.2\mu$  polarization requires a spiral arm field on the order of 10-20 microgauss, to give the required grain alignment, assuming conventional paramagnetic grain models. This field is an order of magnitude stronger than indicated by Zeeman observations. The same difficulty is well-known in studies of visible interstellar polarization, but occurs here at the long wavelengths and over the entire line of sight to the galactic center. Either more efficient alignment mechanisms or cooperative magnetic effects in the grains are indicated.

### Extragalactic Observations

The most clear-cut case of non-thermal polarized infrared emission occurs in BL Lacertae. The visible emission is known to be non-thermal, highly variable, and polarized between 2% and 19%. We observed polarization in BL Lac at  $0.44\mu$ ,  $2.2\mu$ , and  $3.5\mu$  in nearly simultaneous observations (Table 1).

POLARIZATION OF BL LACERTAE

Date (UT) 1976	Wavelength ( $\mu$ )	Flux*	P ± P	σ ± σ
8 June	2.2	0.17 ± 0.03	5.7 ± 0.9	151 ± 5
10 June	3.5	0.31 ± 0.04	10.4 ± 1.7	162 ± 5
11 June	2.2	0.20 ± 0.03	10.0 ± 0.4	171 ± 5
14 June	0.44 (u)	-	2.1 ± 1.0	150 ± 6
14 June	3.5	0.26 ± 0.04	8.6 ± 1.7	158 ± 5
17 June	0.44 (b)	-	8.8 ± 0.4	176 ± 3

\* in units of  $10^{-26} \text{ W m}^{-2} \text{ Hz}^{-1}$

Except for the first entry in the Table, the polarizations are uniform in magnitude and direction. This provides strong evidence that the same mechanism, synchrotron radiation, is operational from the visible to the infrared.

A less clear-cut case is the Seyfert galaxy, NGC 1068. The ultraviolet and visible continua are strongly polarized. R. W. Capps has recently remeasured the  $10\mu$  polarization and found agreement with the earlier results (Table 2) of Knacke and Capps (Ap.J., 192, L19) who argued that non-thermal emission is indicated by the infrared polarization. However, Angel *et al.* (Ap.J., 206, L5) argued that the visible polarization is due to scattering. In that case a dust grain mechanism might be suggested for the infrared polarization also.

POLARIZATION OF NGC 1068 AND THE BN OBJECT

Object	$\lambda(\mu)$	No. of Observations	$P \pm \delta P(\%)$	$\theta \pm \delta\theta(^{\circ})$
NGC 1068.....	3.5	10	$3.2 \pm 0.4$	$88 \pm 5$
	10.2 (Dec.)	15	$2.2 \pm 0.6$	$(52 \pm 16)^*$
	10.2 (Feb.)	6	$2.3 \pm 0.5$	$84 \pm 7$
	18.4	2	$< 4.0 (2\sigma)$	...
BN.....	3.5 (Dec.)	2	$9.4 \pm 1.5$	...
	3.5 (Feb.)	3	$9.4 \pm 0.4$	$114 \pm 2$

It is evident that both dust and non-thermal emission can produce infrared polarization in extragalactic objects. We are continuing these observations to use polarization as a probe of the radiation mechanisms.

INFRARED EMISSION FROM NGC 1068

Roger A. Dana and Vahé Petrosian  
 Institute for Plasma Research  
 Stanford University

The infrared spectrum of the Seyfert galaxy NGC 1068 has recently been extended into the far infrared (30-100 $\mu$ ) by Ricke and Low (1975) and Telesco, Harper and Loewenstein (1976). These observations show a sharp turn-over in the spectrum at 100 $\mu$  and roughly a power law spectrum between 10 and 100 $\mu$ . Together with the millimeter upper limits of Kellermann and Pauling-Toth (1971) and Elias, et al (1975) and the near infrared observations of Jameson, et al (1975), Simon and Dyck (1975), and Neugebauer, et al (1971), the qualitative shape of the infrared spectrum is now apparent.

Using approximate solutions of radiative transfer (Petrosian and Dana 1975) and of infrared emission (Dana and Petrosian 1976) we examine the possibility of dust emission as the source of the infrared radiation. We constrain our models to match both the H $\beta$  luminosity ( $L_{H\beta} = 3 \times 10^{41}$  ergs/sec, Shields and Oke 1975) and the infrared luminosity ( $L_{IR} = 1.75 \times 10^{45}$  ergs/sec, Telesco, et al 1976). We also require that the Strömngren radius be 50 pc. Thus most of the line emission will come from a region  $\sim 1''$  in diameter ( $\sim 100$ pc for  $D = 22$  Mpc) as observed by Shields and Oke (1975).

For an assumed spectrum of ionizing radiation (or a parameter  $\gamma_c$ , the ratio of the number of hydrogen ionizing photons to the total number of photons from the central source), the ratio  $L_{H\beta} / L_{IR}$  fixes the dust optical depth at optical and ultraviolet wavelengths. The spectrum of the infrared radiation then depends on the radial variation of the dust density and on the ratio of infrared emissivity to ultraviolet opacity of the dust grains, or a parameter  $Q$  defined as

$$Q = \kappa_d(\lambda_o) / \epsilon_{IR}(\lambda_o), \quad \lambda_o = 912\text{\AA}$$

$\kappa_d(\lambda_o)$  is the opacity of dust at the Lyman limit and  $\epsilon_{IR}(\lambda)$  is the infrared emissivity of dust and is defined as

$$\epsilon_{IR}(\lambda) = \pi a^2 (2\pi a / \lambda)^j .$$

For normal interstellar dust,  $Q$  is of the order of unity.

Our fits assume that the dust is optically thin in the infrared. Only in the case that the dust is optically thick over a significant portion of the infrared spectrum will self absorption affect the dust temperature because dust heating is dominated by absorption of ultraviolet photons. A silicate absorption feature is present (Kleinmann, et al 1976) with an optical depth  $0.4 < \tau(9.7\mu) < 1.2$ , but we have neglected this in our calculations.

In general we find it difficult to fit the  $100\mu$  data along with the data at shorter wavelengths with reasonable dust distributions. Even neglecting the difference between the observations at  $100\mu$  and the model predictions, we find that in order to obtain the high observed intensity at  $40$  to  $50\mu$  from dust located so close to the central source, we must postulate the existence of grains which cool off very efficiently via infrared emission. In other words, the derived parameter  $Q$  is unreasonably low.

The required values of  $\gamma_c$ ,  $j$ , dust-to-gas ratio and the dust and gas distribution for the best fits will be presented.

This work was partially supported by the NASA-Ames University Interchange Agreement NCA2-OR745-613.

#### REFERENCES

- Dana, R. A., and Petrosian, V. 1976. In preparation.
- Elias, J. H., Gezari, D. V., Hauser, M. G., Neugebauer, G., Werner, M.W., Westbrook, W. E. 1975, paper read at the 146th Meeting of the AAS, San Diego, California, 1975 August 17-20.
- Jameson, R. F., Longmore, A. J., McLinn, J. A., and Woolf, N. J. 1974, Ap. J. 190, 353.
- Kellermann, K. I., and Pauling-Toth, I. I. K. 1971, Ap. J. Letters, 8, L153.
- Kleinmann, D. E., Gillett, F. C., and Wright, E. L. 1976, Ap. J. 208, 42.
- Neugebauer, G., Garmire, G., Rieke, G. H., and Low, F. J. 1971, Ap. J. Letters, 166, L45.
- Petrosian, V. and Dana, R. A. 1975, Ap. J. 196, 733.
- Rieke, G. H. and Low, F. J. 1975, Ap. J. Letters, 199, L13.
- Shields, G. A. and Oke, J. B. 1975, Ap. J. 197, 5.
- Simon, T. and Dyck, H. M. 1975, M.N.R.A.S. 172, 19P.
- Telesco, C. M., Harper, P. A., and Loewenstein, R. F. 1976, Ap. J. Letters, 203, L53.